X-RAY PEAK AREA AS A METHOD OF CHARACTERIZING PETROLEUM COKES

V. Dean Allred

Marathon Oil Company
Denver Research Center
P. O. Box 269
Denver, Colorado 80120

OVERVIEW

X-ray diffraction analysis is a versatile tool in the characterization of petroleum coke. In 1963 personnel at Marathon's Research Center worked out a procedure where X-ray diffraction analysis of a coke sample could be used to classify it broadly with respect to the linear CTE (Coefficient of Thermal Expansion) value of graphite which would be produced by it.[1] This technique was based on the observation that a plot of the CTE versus the logarithm of the ratio of peak height to width at one-half height gave a reasonably straight line function. Calibration was by comparison to a series of standard samples.

Success of the procedure depended on firing a sample to the same conditions of time and temperature. Initially, samples of the standards were fired simultaneously with the unknown and excellent results were obtained. However, as the supply of standard cokes was depleted, it was evident that some other procedure was needed. Therefore, a series of standard fired samples were prepared. These standards were then to be used over and over again as calibration standards. The critical operations then became the technique for preparing the unknown samples and the mounting of individual samples in the holder of the X-ray diffraction unit. The most sensitive item was the calcining procedure since both the peak height and width were strongly dependent on the firing history (temperature and time at temperature). That is, over the calcining temperature range, as the firing temperature was increased the peak height (intensity) increases exponentially, and the peak width to a lesser degree decreases in a similar manner.

At an early date it was recognized that for almost all delayed petroleum cokes, the average peak width was almost a unique function of the firing history and not much affected by the coke type. Whereas, the peak height was extremely sensitive to the coke type for comparable firing conditions. The average peak width, therefore, could be used as an indicator of the correct firing history. Comparing the peak width for the unknown with that of the standard samples indicated whether the X-ray data was suitable for a CTE correlation.

Experience soon showed that it was difficult to adequately reproduce firing conditions. This problem led to a re-evaluation of the X-ray peak width and height relationships to determine if correction factors could be applied to bring the data in line or whether some other relationship could be found. As a result, it was discovered that the peak height times the average peak width (in consistent X-ray units) was remarkably constant over a fairly broad temperature range (~ 2400 to 2600°F). Whereas, the ratio of peak height over width was actually changing exponentially (Figure 1). Fortunately, this constant area region also coincided with the temperature range where petroleum cokes are usually calcined. Therefore, the extreme care used in firing of cokes for X-ray/CTE correlation is now unnecessary, the accuracy of the correlation has improved, and it is possible to evaluate cokes calcined by others, e.g., in commercial calciners.

EXPERIMENTAL

Sample Preparation

Assuming that the firing of the coke sample has been within the required temperature limits, the most critical item of sample preparation becomes the operator's technique in packing or loading the sample holder. However, sample preparation consistent with good X-ray diffraction analysis must also be practiced, i.e., obtaining a representative sample and reduction to X-ray sample size.

Loading of the sample in the holder is critical since some preferred orientation can be given to the coke -- particularly for low CTE cokes, which will influence the intensity of the diffraction peak. Good reproducible results, therefore, depend on the experience and care used by the operator in loading and operating his equipment so that it is done the same way each time. (In our laboratory, samples used as calibration standards are reloaded each time as part of the procedure.) If the calibration data are essentially constant for successive determinations, one can be relatively sure that the data from the unknown will also be consistent. It is also good practice for the spectroscopist to run a minimum number of determinations (usually two or three) for the sample and the standards to see that the data are self consistent.

Data Evaluation

The only X-ray diffraction peak that has proven valuable for characterizing delayed petroleum cokes fired in a temperature range up to 3000°F is the 002 graphite line. A typical trace showing this peak is given as Figure 2. In obtaining the required data, the peak height (H) and width at half-height ($\beta_{1/2}$) are taken from the chart in terms of linear measurement, however, it should be noted that they do not represent consistent units. That is, the peak width is caused by scattering and is a function of the size of the diffracting crystallites. It has the units of angular scan (2θ) in degrees, as determined by the geometry of the goniometer being used. Peak height on the other hand is a measure of the intensity of the diffracted X-ray radiation. Normally, it is measured by a radiation counter and has the dimensions of so many counts per unit of time.

In making an X-ray evaluation of petroleum coke for correlation purposes, it is therefore necessary to use fixed operating conditions. Further, it is questionable whether data from one X-ray unit should ever be compared directly with that of another. On the other hand, through the use of the calibration standards, differences between two different X-ray units can be readily resolved, and data correlated accordingly.

Finally, it is also recognized that the peak width has in it a factor caused by inherent scattering due to the instrument itself. This is usually quite small and remains constant if the alignment of the X-ray unit does not change. In calculating crystallite size it is important to correct for the machine scattering factor (β_o). However, in making these correlations, the experimental width has been used directly since a change in β_o would be indicated by a change in the value determined for the calibration standard.

DISCUSSION

Temperature Effects

Firing temperatures in excess of 2000°F are desirable for the X-ray/CTE correlations. The temperature sensitivity of the peak height and width for a typical petroleum coke is shown in Figure 3. As indicated in this figure, some anomalies exist in the X-ray data for coke fired at temperatures below 1800°F. The anomalous behavior is particularly noticeable in the average peak width in that it at first increases and then reverses itself and decreases with temperature. The peak height on the other hand remains almost constant through this particular temperature range. The low temperature anomaly in peak width is probably indicative of a structural change as the carbonaceous polymer (green coke) decomposes to form carbon. (The helium density also undergoes an anomalous change in the temperature range 1400 to 1600°F.)

Time Effects

The firing history of calcined petroleum coke depends on temperature and time at temperature. The peak width function most nearly reflects the firing history. The temperature has a greater effect than time, nevertheless, time at temperature can be an important variable particularly when short-time periods are involved.

Figures 4a and 4b show the change in 002 peak width and height, respectively, as a function of time for samples of a typical petroleum coke heated at a constant temperature for various periods of time. For convenience, these data are plotted with the reciprocal of time as a coordinate since the change in the width function decreases rapidly with time and approaches a limiting value at infinite time. The coke used in these determinations had been previously devolatilized at 1800°F ($\beta_{1/2} \sim 3.00$) to stabilize them. In obtaining the data, the coke samples (in graphite crucibles) were placed in a preheated oven and allowed to come up to temperature (about 30 minutes) before timing commenced. At predetermined times individual crucibles were withdrawn and cooled under a carbon dioxide atmosphere.

Figure 4c shows the relationship between peak area and the calcining time. These data show -- even with appreciable scatter of data points -- that the peak area is independent of time-temperature relationship over a considerable range (2400 to 2600°F over times from 5 minutes to 24 hours).

Relationship of Coke Type

Figure 5 is a plot of the average peak width versus peak area obtained for coke samples produced from vacuum residuum, topped crude oil, and thermal tars. (CTE range from 4 to 30 [x 10^{-7}]). As previously noted, the width is relatively independent of the delayed coke type (i.e., high or low CTE). On the other hand, the height -- and subsequently the area -- is strongly affected by the coke type. Nevertheless, the product of the width by the height ($H\beta_{1/2}$) remains characteristically constant for a given coke type over the same range of peak width ($\beta_{1/2} \sim 1.25$ to 1.75).

The X-ray/CTE Correlation

Figure 6 shows a plot of the X-ray peak area versus the CTE factor obtained for graphite produced from it for coke used as calibration samples. Experience gained during the past several years has shown that most delayed petroleum cokes will produce graphite with a CTE value comparable to its relative position on such a calibration curve.

SUMMARY

A technique to determine an X-ray/CTE correlation factor for calcined petroleum coke has been developed. This procedure permits classification of a petroleum coke as to its potential use and value without having to prepare a graphite test specimen.

REFERENCE

1. Stout, C. F., Janes, M., and Biehl, J. A., "Research and Development on Advanced Graphite Materials", p. 20-23, XXXVI Technical Documentary Report WADD TR 61-72, August, 1964, U.S.A.F. Systems Command, Wright-Patterson Air Force Base, Ohio.

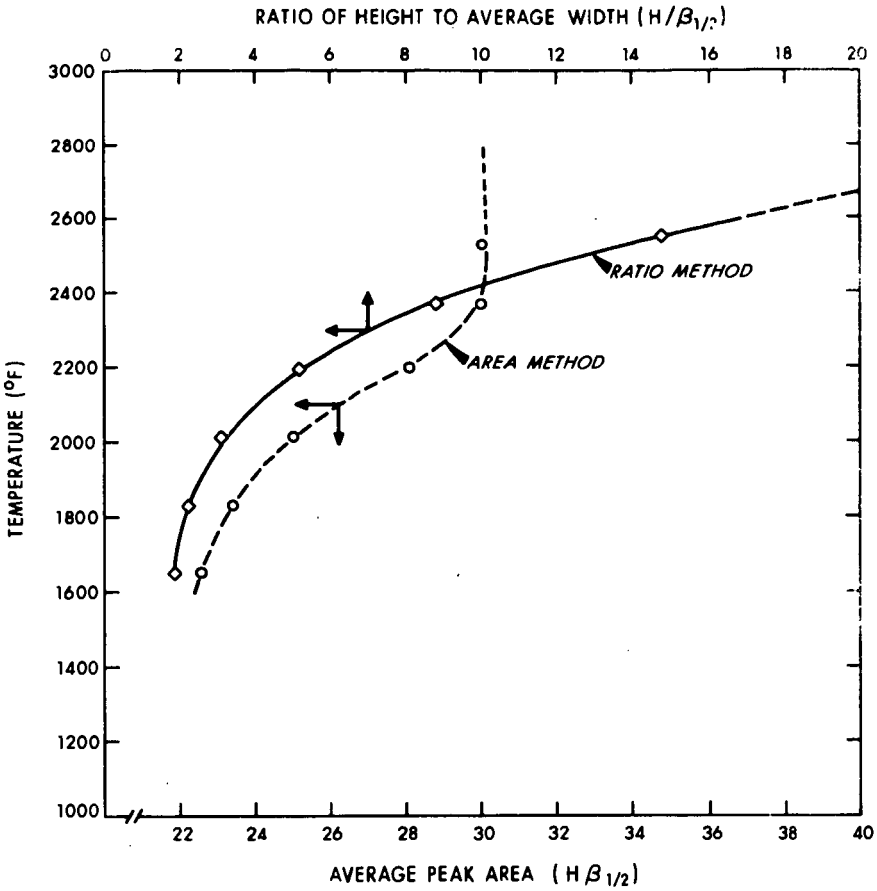

FIGURE 1. DATA SHOWING THE TEMPERATURE SENSITIVITY OF THE 002 X-RAY PEAK HEIGHT VS WIDTH AT ONE-HALF HEIGHT AS A RATIO AND AN AREA.

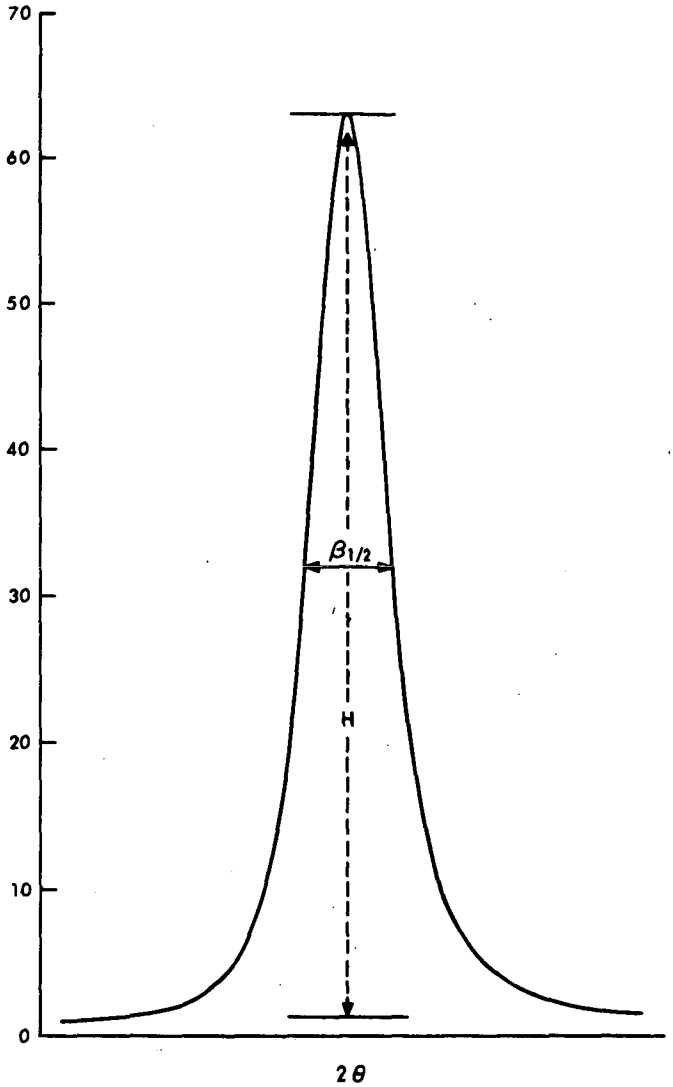

FIGURE 2. TYPICAL CHART TRACE SHOWING THE 002 DIFFRACTION LINE.

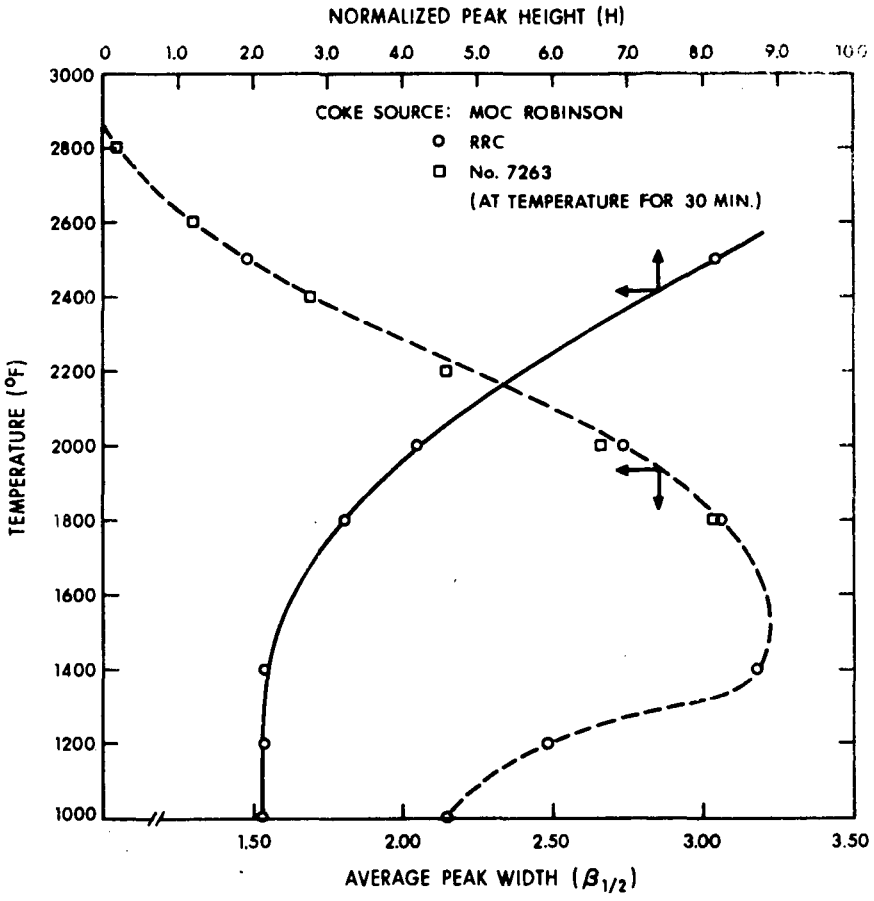

FIGURE 3. TEMPERATURE SENSITIVITY OF AVERAGE PEAK WIDTH ($\beta_{1/2}$) AND PEAK HEIGHT (H).

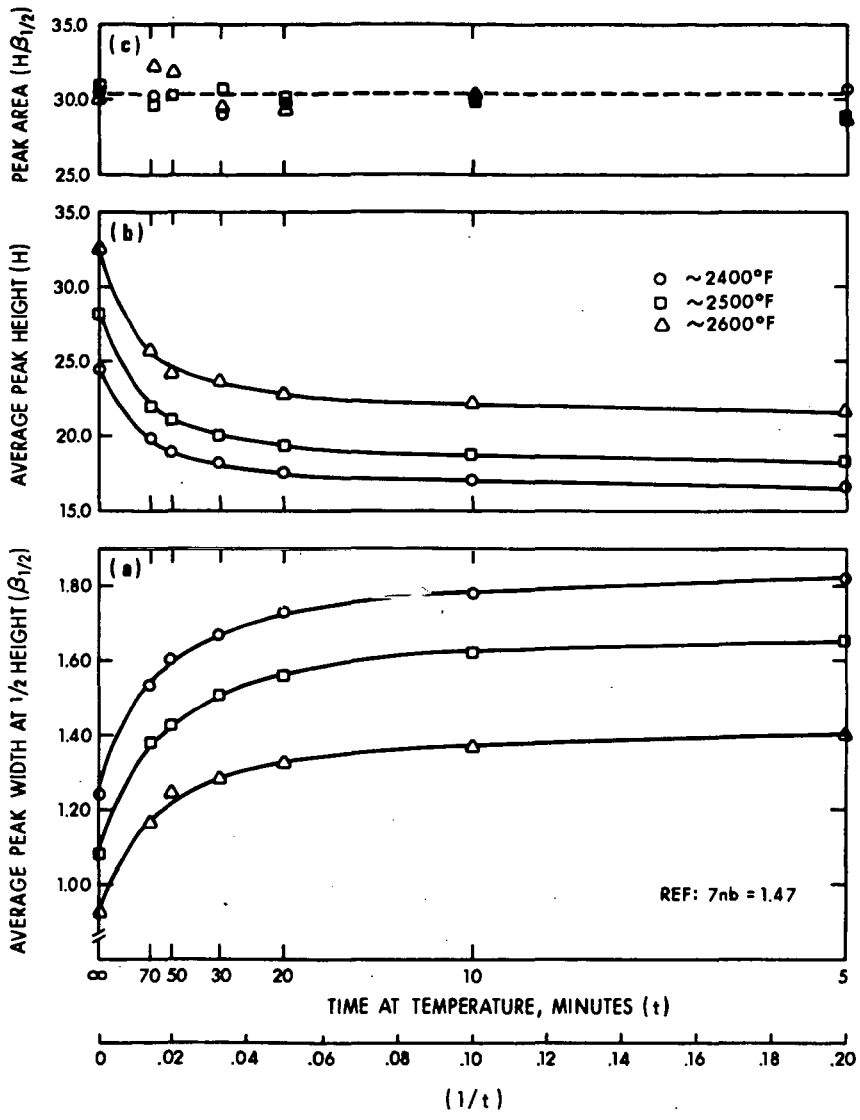

FIGURE 4. a-c. TIME-TEMPERATURE EFFECTS WITH AVERAGE PEAK WIDTH, PEAK HEIGHT, AND AREA.

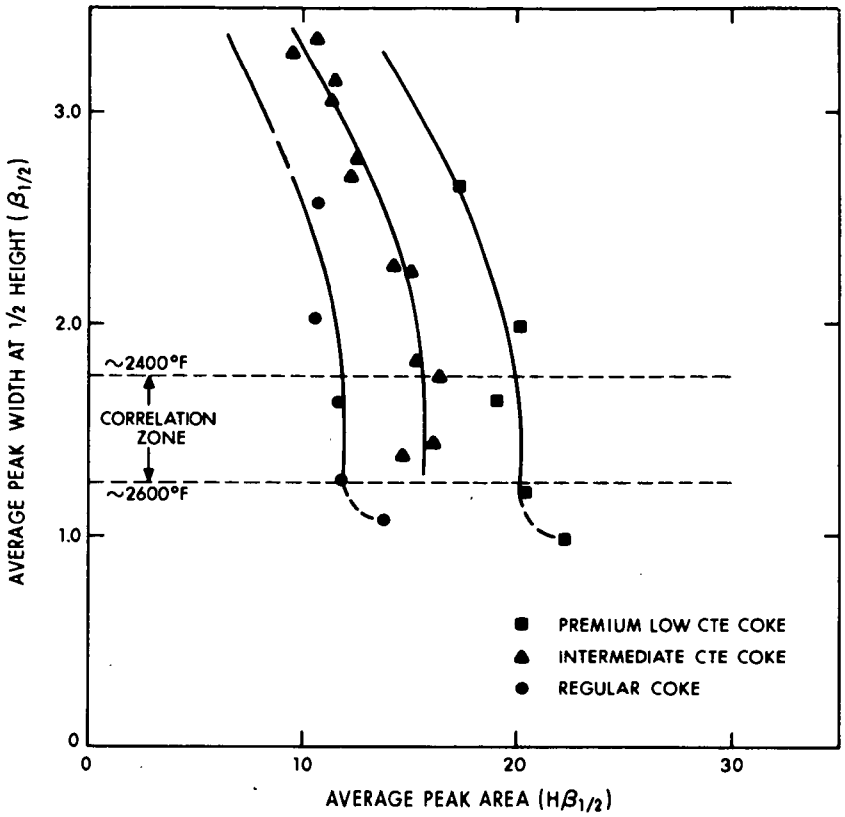

FIGURE 5. RELATIONSHIP BETWEEN COKE TYPE AND AREA AS A FUNCTION OF AVERAGE PEAK WIDTH.

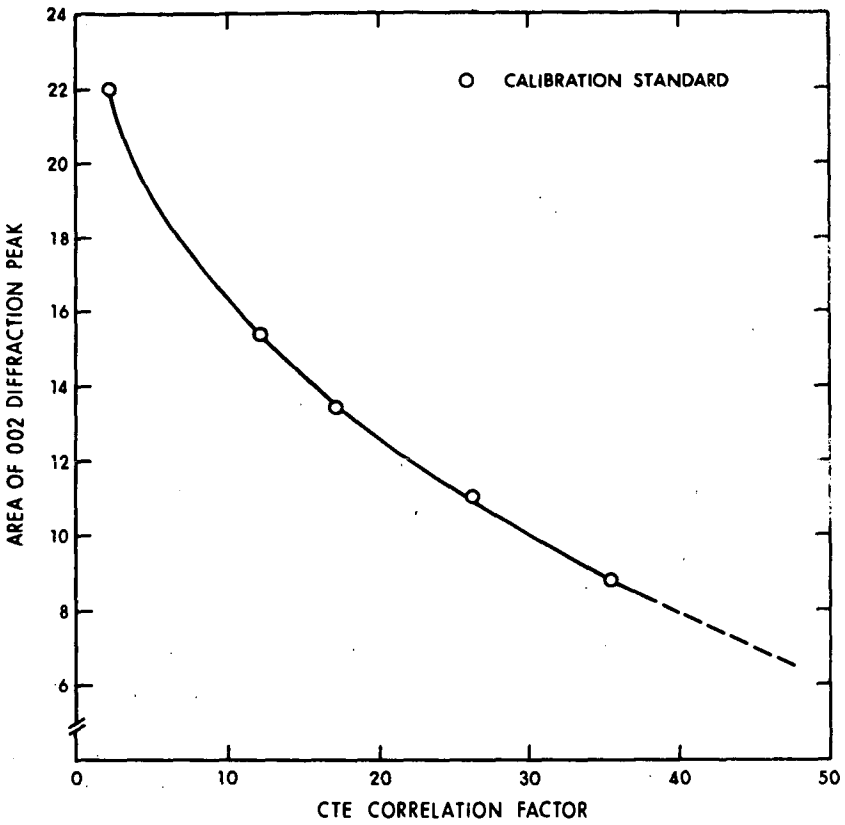

FIGURE 6. TYPICAL CTE/X-RAY CORRELATION CALIBRATION CURVE.

KINETICS OF CARBON DIOXIDE METHANATION ON A RUTHENIUM CATALYST

Peter J. Lunde and Frank L. Kester

Hamilton Standard Division,
United Aircraft Corporation
Windsor Locks, Connecticut, 06096

INTRODUCTION

The catalytic hydrogenation of carbon dioxide to methane

$$4H_2(g) + CO_2(g) \rightleftharpoons CH_4(g) + 2H_2O(g) + 43 \text{ Kcal}$$

is often called the Sabatier reaction, after the Belgian chemist who investigated the hydrogenation of hydrocarbons using a nickel catalyst. The Sabatier reaction is becoming of commercial interest for the manufacture of natural gas from the products of coal gasification. The reverse reaction, of course, is called steam reformation and is a commercial method for hydrogen manufacture.

This paper developed from work performed under contract to NASA to investigate the Sabatier reaction as a step in reclaiming oxygen within closed cycle life support systems. Carbon dioxide from the cabin atmosphere is thus changed into water vapor which is electrolyzed to provide oxygen for the cabin plus one-half the hydrogen required for the Sabatier reaction. The rest of the hydrogen is provided from the electrolysis of stored water, which produces breathing oxygen as a by-product, reducing the proportion of available carbon dioxide which must be reacted and assuring excess carbon dioxide in the feed mixture.

The Sabatier reaction is a reversible, highly exothermic reaction which proceeds at a useful rate at the low temperatures required for high yields only when a catalyst is used. Dew, White, and Sliepcevitch (1) studied this reaction using a nickel catalyst. This paper examines the kinetics of the reaction using a Ruthenium catalyst, and derives from experimental data a correlation describing the kinetics of this catalysis in the 400°F to 700°F temperature range.

Thermodynamics

Equilibrium compositions for hydrogen and carbon dioxide mixtures at 1 atm are shown in Figure 1, which was prepared with the aid of a computer program developed by United Aircraft Research Laboratories using free energies from Wagman (2). Carbon and carbon monoxide are possible products, as well as methane and water vapor. The reaction proceeds as written

$$4H_2(g) + CO_2(g) \rightleftharpoons 2H_2O(g) + CH_4(g)$$

for molar feed ratios (H_2:CO_2) of over 3.5:1 at temperatures from 400°F to 700°F.

Low temperatures favor high conversions. At 700°F and a feed ratio (H_2:CO_2) of 3.5:1 the equilibrium conversion of H_2 is only 90%, while at 400°F it is about 99%.

As the feed ratio falls below 3.5:1, carbon becomes thermodynamically stable at higher and higher temperatures. At 3:1, carbon deposition is possible only below 500°F while at 2:1 it is stable below 1100°F.

Carbon monoxide formation is thermodynamically possible above 700°F, where the reaction encounters the well-known "water gas shift".

$$CO_2 + H_2 \rightleftharpoons CO + H_2O$$

This does not cause a limitation in maximum operating temperature because any carbon monoxide formed is converted to other products downstream in the reactor's subsequent 400°F - 700°F temperature zone which is necessary for a practical yield.

EXPERIMENTAL

Catalyst Selection

Thompson (3) conducted a Sabatier catalyst screening program for the US Air Force. Four catalysts were experimentally evaluated:

1) Nickel (80% Ni and NiO) on kieselguhr)
2) 0.5% ruthenium (on alumina)
3) 0.5% rhodium (on alumina)
4) 0.5% cobalt (on alumina)

Ruthenium and nickel were found to be appreciably more active catalysts for promoting the Sabatier reaction. Nickel, however, presented several operating problems.

1) Slow deterioration over the test period, attributed to sulfur poisoning.
2) Reactor startup in hydrogen was advisable to assure reduction of nickel to its most active form.
3) Carbon deposition was reported at 650°F to 700°F.

Ruthenium had none of these problems, and was somewhat more active than the nickel as a catalyst. Furthermore, there was a potential for even more activity if heavier loadings of the metal on the substrate are used.

Consequently a 0.5% ruthenium catalyst on 1/8 in x 1/8 cylindrical alumina pellets was selected for further investigation. The prepared catalyst, Englehard type "E", was purchased from

Englehard Industries Division
Englehard Minerals and Chemicals Corp.
113 Aster Street
Newark, N. J.

The manufacturer furnished no lot number or other specific information but did disclose that the catalyst performed within the limits of their internal specifications. Superficial examination of the pellets indicated the ruthenium did not penetrate more than 1/2 mm into the alumina indicating that pore diffusion was not likely to be important in the performance of this catalyst. The bulk density of the pellets was measured as 1.0 g/cc.

Approach

The ruthenium catalyst is relatively new and there are no published quantitative data from which the kinetics can be determined. Consequently, an experimental apparatus was designed and a program to acquire rate data was begun.

Hydrogen and carbon dioxide were fed continuously to the experimental apparatus. The test reactor, a tube filled with catalyst and held isothermal by immersion in a molten salt bath, was made small so that the conversion of unreacted feed was low but measurable at the lowest operating temperature, minimumizing the reaction heat released. At higher temperatures part of the feed was passed through a large "supply" reactor providing a partly reacted feed to the test reactor which reduced the reaction rate and the reaction heat released.

Steady state conversions were determined from flow information and chromatographic analyses of the test reactor inlet and outlet streams. Mass flow to the reactor was held steady for runs at several temperatures, giving data for calculation of the reaction activation energy, which describes the temperature dependence of the reaction rate. Additional runs were made at constant temperature to determine the basic reaction rate constant.

Feed flow ratios (H_2:CO_2) of 2:1 and nearly 4:1 were investigated. Temperatures of 400°F to 700°F were selected for activation energy data accumulation since at temperatures over 700°F the reaction proceeds rapidly and is complicated by carbon dioxide formation, while 400°F is low enough to allow virtually complete conversion of the feed in a practical reactor.

Apparatus

A schematic for the complete experimental rate data apparatus is shown in Figure 2.

The feed rates of hydrogen and carbon dioxide were set externally using laminar flowmeters. Electronic differential pressure sensors converted a differential pressure flow signal to an electrical voltage which was read on a digital voltmeter. The flowmeter calibrations are shown in Figure 3.

When desired, partially reacted feed was produced by passing part of the mixed feed flow through a "supply" Sabatier reactor. This reactor, which also used a ruthenium catalyst, was heated to about 650°F and was large enough to react 80% - 90% of the stoichiometrically lean feed constituent.

Sampling

All samples except the inlet feed were fed to a Bendix process chromatograph at very low flow (Figure 2, S1, S2, S4, S5). The inlet feed sample (S3) was taken by actuating two three-way valves which directed the entire feed stream through the chromatograph sampling valve. A sample could be taken in this manner without changing the feed flow rate. When other samples were being taken the pressure drop of the chromatograph sampling valve (about 0.6 - 0.8 psi) was simulated in the feed line with a precision metering valve (marked "ADJ") set to maintain a constant pressure at PI-2 so that there was no transient when the feed sample valves were actuated. Heating tape and heated valve boxes were necessary throughout the sampling system to prevent water from condensing in the sample lines.

The process gas chromatograph analyzed feed and effluent gases using samples of equal volume for analysis. Peaks were automatically gated, attenuated and

recorded. Peak heights were then manually measured and logged as raw composition data. Components analyzed were H_2O, CO_2, H_2, CO, CH_4, N_2, Ar, and O_2, but the last three were not present in significant quantities. A typical chromatogram is shown in Figure 4. Each analysis took 13 minutes and was always repeated before data was recorded.

The chromatograph was calibrated by using pure CO_2, H_2, and CH_4, at several pressures in the 0-1 atm range. The chromatographic peak heights then corresponded to partial pressures of the calibrated constituents. Water was calibrated indirectly using Sabatier reactor effluent, in which the partial pressure of water vapor was necessarily exactly twice that of the methane which was already calibrated. Final calibration curves for the chromatograph are shown in Figure 5.

After the chromatograph was calibrated, the hydrogen peak signal became erratic during the data collection phase. Successful gas analyses were continued by taking the correct hydrogen partial pressure as equal to the difference between analysis pressure and the sum of the other constituents as determined from their peak heights and calibration curves. The accuracy of this method was confirmed later in this work after the electronic malfunction responsible was repaired.

Test Reactor

The differential reactor used for the actual kinetic study was made from 1/2 in. stainless steel tubing (0.43 in ID x 1.75 in). The catalyst charge of 3.58 grams (about eighty 1/8 in. x 1/8 in. cylindrical alumina pellets coated with 1/2% ruthenium) filled the 4.15 cc reactor tube. The reactor was called the "differential" reactor because its purpose was to convert only a small portion of the feed stream to the Sabatier products.

The differential reactor assembly, consisting of a feed preheating coil, thermocouples and sample tubes (Figure 6) was submerged in an oven-heated molten salt bath to keep the reactor isothermal, because of the high heat of reaction. Thermocouples were installed in the inlet stream (T2), outlet stream (T4), at the center of the reactor (T3), and on the reactor wall (T5). Samples could be taken from the feed (after preheat) (S4), effluent (S5), and (externally) from the feed before entering the reactor.

At the low end of the temperature range (400° - 500°F) reaction rates were low and the reactor wall and center thermocouples agreed $\pm$ 1°F. At higher temperatures the reaction rate was high and the reaction rate was reduced so that the temperature differential was held below 10°F by partly reacting the inlet feed before it entered the differential reactor. Using this technique good experimental data could be taken from 400°F to 700°F in a single reactor with a constant feed rate.

DISCUSSION

Since the mechanism for ruthenium catalysis is unknown, gas phase type kinetics are proposed for the reaction:

$$4H_2(g) + CO_2(g) \underset{kr}{\overset{kf}{\rightleftharpoons}} 2H_2O(g) + CH_4(g)$$

where k_f and k_r represent reaction rate constants for the forward and reverse reactions, respectively. Thus

$$-\frac{d\left[P_{CO_2}\right]}{dt} = k_r^n \left[P_{H_2O}\right]^{2n} \left[P_{CH_4}\right]^n - k_f^n \left[P_{CO_2}\right]^n \left[P_{H_2}\right]^{4n} \qquad (1)$$

where n is an emperical constant equal to 1 for pure gas phase kinetics.

When equilibrium is achieved, $-d\left[P_{CO_2}\right]/dt = 0$, and equation (1) becomes

$$K_e = \frac{k_f}{k_r} = \frac{\left[P_{H_2O}\right]^2\left[P_{CH_4}\right]}{\left[P_{CO_2}\right]\left[P_{H_2}\right]^4} \qquad (2)$$

and the emperical exponent applied to the exponential coefficients cancels so that the equilibrium constant, K_e, is defined as a classical thermodynamics.

Noting the $K_e^n = k_f^n/k_r^n$, if equation (1) is rewritten (3)

$$-\frac{d\left[P_{CO_2}\right]}{dt} = k_f^n \left\{ \left[P_{CO_2}\right]^n\left[P_{H_2}\right]^{4n} - \frac{\left[P_{CH_4}\right]^n\left[P_{H_2O}\right]^{2n}}{(Keq(T))^n} \right\} \qquad (4)$$

then the temperature dependence of the reaction rate constants can be described by the general Arrhenius relationship

$$k_f^n(T) = k \exp(-E_a/RT) \qquad (5)$$

and thus the final form of the rate expression is

$$-\frac{d\left[P_{CO_2}\right]}{dt} = k \exp(-E_a/RT) \left\{ \left[P_{CO_2}\right]^n\left[P_{H_2}\right]^{4n} - \frac{\left[P_{CH_4}\right]^n\left[P_{H_2O}\right]^{2n}}{(Keq(T))^n} \right\} \qquad (6)$$

where k (the rate constant) and Ea (the activation energy) and n (catalyst coefficient) are constants to be determined for the experimental data.

To find the activation energy E_a and catalyst coefficient n for equation (6) the logarithms of both sides are taken. Rearrangement then gives

$$Y \equiv \ln \frac{-d\left[P_{CO_2}\right]/dt}{\left[P_{CO_2}\right]^n\left[P_{H_2}\right]^{4n} - \frac{1}{Keq^n}\left[P_{CH_4}\right]^n\left[P_{H_2O}\right]^{2n}} = \left[\frac{Ea}{R}\right]\left[\frac{1}{T}\right] + \ln k \qquad (7)$$

which is of the form $Y = mX + b$. A plot of Y vs 1/T thus has a slope of Ea/R, enabling determination of Ea. The catalyst coefficient n can be determined by trial because improper values of n do not give a linear plot of experimental data.

With Ea and n determined, equation (6) can be now integrated to obtain a value of rate constant k for each experimental run.

Rearranging and solving equation (6) for k

$$k = e^{-Ea/RT}\left[\frac{dP_{CO_2}}{dt}\right]\left[\frac{-1}{\left[P_{CO_2}\right]^n\left[P_{H_2}\right]^{4n} - \frac{1}{K_{eq}^n}\left[P_{CH_4}\right]^n\left[P_{H_2O}\right]^{2n}}\right] \qquad (8)$$

If the change in P_{CO_2} as it passes through the reactor is defined as X, then the variables can be separated

$$k = e^{-Ea/RT} \frac{dX}{dt} \left[\frac{-1}{\left[P^{in}_{CO_2} - X\right]^n \left[P^{in}_{H_2} - 4X\right]^{4n} - \frac{1}{K_{eq}^n} \left[X\right]^n \left[2X\right]^{2n}} \right] \quad (9)$$

where $P^{in}_{CO_2}$ and $P^{in}_{H_2}$ are inlet partial pressures.

Integrating equation (9) from reactor inlet to outlet,

$$k = e^{-Ea/RT} \frac{\int_0^{P^{in}_{CO_2} - P^{out}_{CO_2}} \frac{dX}{\left[P^{in}_{CO_2} - X\right]^n \left[P^{in}_{H_2} - 4X\right]^{4n} - \frac{1}{K_{eq}^n} \left[X\right]^n \left[2X\right]^{2n}}}{\int_{t_{in}}^{t_{out}} dt} \quad (10)$$

Since space velocity $S_v = \frac{1}{t}$ where t is contact time,

$$k = e^{-Ea/RT} S_v \int_0^{P^{in}_{CO_2} - P^{out}_{CO_2}} \left[\frac{dX}{\left[P^{in}_{CO_2} - X\right]^n \left[P^{in}_{H_2} - 4X\right]^{4n} - \frac{1}{K_{eq}^n} \left[X\right]^n \left[2X\right]^{2n}} \right] \quad (11)$$

The integral involves only inlet and outlet concentrations, known kinetic constants and the running variable X, and can be solved by numerical or graphical techniques. Values of $K_{eq}(T)$ were obtained from (2).

A standard fourth order Runge-Kutta numerical integration technique was carried out for each test run using a computer program written explicitly for this work. The Runge-Kutta method, which employs a Taylor series expansion of the derivative function, was selected because of its accuracy and stability (4).

RESULTS

Two series of data were taken using the differential test reactor. The activation energy series was run over a wide temperature range at low reaction rates to determine activation energy and catalyst coefficient. The reaction rate series was run at a single temperature and varying reaction rates to determine the reaction rate coefficient.

Table I shows the complete experimental data after preliminary processing.[1] Table II shows the results of activation energy calculations from equation (7) using selected runs. Table III shows the results of integration of other selected runs to calculate a rate constant according to equation (11). Table IV indicates the criteria for selecting runs for these calculations.

The activation energy series was started at 400°F and the temperature gradually raised to 700°F while the conversion of the inlet gas was raised from 0% to 96% to keep the composition change across the differential reactor small (Runs 519-551). Volumetric flow of the feed gas was held steady except for two lower value runs at the start. The ratio of H_2:CO_2 in the feed gas was held just below stoichiometric (at 3.8) for the first temperature sweep (Runs 519-534), and at about 2.0 for the second (Runs 538.50 - 551).

The reaction rate series was run at bath temperatures of 580°F and 520°F and at inlet flow ratios of 1.9 and 2.9, respectively (Runs 560-581). Inlet conversions were varied from 0% to 84%. Two final runs were taken at flow ratios just over stoichiometric (at 4.1) using lower bath temperatures providing unreacted feed gas at 435°F and 475°F (Runs 590 and 591).

The lower inlet flow ratios of H_2:CO_2 in each series was within the range for which carbon deposition was thermodynamically stable (Figure 1). No evidence for such deposition was observed in these tests in performance degradation or after post-test catalyst examination.

EXPERIMENTAL DATA REDUCTION

A data reduction computer program was used to produce the data presented in Table I.

Inlet and Outlet Partial Pressures - Inlet analysis total pressure was taken as the arithmetic average between supply reactor pressure (PI-2, Figure 2) and differential reactor inlet pressure (PI-3). CO_2, H_2O, and CH_4 partial pressures were determined from chromatographic peak heights and H_2 taken as the remaining constituent by difference, as discussed in "Sampling", above. The partial pressures were then normalized to total 1.000, thus becoming mol fractions, and then mutiplied by the inlet reactor pressure (PI-3) to determine inlet partial pressures*.

The experimental outlet compositions were determined similarly, except that the analysis pressure was taken as the arithmetic average between differential reactor outlet (PI-4) and chromatograph outlet (PI-5). After mol fraction calculation, a new stoichiometrically exact set of outlet mol fractions was synthesized from the inlet compositions plus the outlet CH_4 composition[2]. The synthesized values were printed next to the experimental values for easy comparison. Generally the values agreed within a factor of 1%, and often the agreement was much better. Constituent outlet partial pressures* were then calculated from the synthesized outlet composition and outlet reactor pressure.

Reactor Flow Rates - Laminar flowmeter voltages were converted to total volumetric inlet flow* and then weight flow (lb/hr) using flowmeter pressure, temperature, and the perfect gas laws. Volumetric flow rates for each constitutent were then

---

[1]Complete raw data is given in Reference 5, which is the NASA report of this work.
*Presented in Table 1 for all reported test runs.
[2]This was done to avoid errors in later calculations due to experimental inaccuracies.

calculated at reactor inlet and outlet, taking into account the reactor temperature*, pressure, and chromatographically determined compositions while conserving only the total weight flow of the feed constituents. Contact time (sec) and space velocity* (1/hr) were calculated using the reactor volume* and average reactor flow rate. Reactor inlet and outlet flows in lb-mols/hr were then calculated, using volumetric flows and the perfect gas laws.

Reaction Rates - Molar CO_2 reaction rate (lb-mol/hr) was then calculated from the difference in inlet and outlet molar flow rates of CO_2. Then the specific conversion rate was calculated (lb-mol/hr catalyst), using catalyst weight*.

CO_2 reaction rate* in atm/hr was also calculated, using the perfect gas law at reaction conditions and the molar reaction rate.

DATA CORRELATION

Reduced run data listed in Table I was further processed to determine values of the activation energy, Ea, catalyst coefficient, n, and reaction rate coefficient, k.

Activation Energy and Catalyst Coefficient - A specail computer program was written to process reduced data from the activation energy runs to a form appropriate for graphically fitting equation (7). A least squares fit was incorporated to calculate the activation energy directly. Table II is an output from this program for n = 1/4. The data were fitted using catalyst coefficients of n = 1/4, 3/8, 1/2, and 1. When n was 1/4 or 3/8, a plot of equation (7) was generally linear (Figures 7 and 8). The data were more linear with n = 1/4 and this was selected as the catalyst coefficient, resulting in a value for activation energy of

$$Ea = 30{,}600 \quad \text{btu/lb mols } CO_2$$

or

$$Ea = 17.0 \quad \text{Kcal/g mols } CO_2$$

Rate Coefficient - Table III is the output from the Runge-Kutta integration routine which calculates the rate constants for selected runs according to equation (11). Data for integration were selected as noted in Table IV.

The required program input for the data reduction is tabulated along with the calculated rate constant for each run. The average constant is

$$k = 2.46 \times 10^9 \ \text{atm}^{-1/4} \ \text{hr}^{-1}$$

for the constant temperature runs 544.1 to 581.0 and

$$k = 2.338 \times 10^9 \ \text{atm}^{-1/4} \ \text{hr}^{-1}$$

for the entire page of tests of Table IV.

*Presented in Table I for all reported test runs.

References

1. Dew, J. M., White, R. R. and Sliepcevitch, C. M. "Hydrogenation of Carbon Dioxide on a Nickel - Kieselguhr Catalyst". IEC V 47, 1, Jan. 1955 p. 140-146.

2. Wagman, D. D., et al "Heats, Free Energies, and Equilibrium Constants of Some Reactions involving O_2, H_2, H_2O, C, CO, CO_2, and CH_4". Research Paper RP 1634, J. Res. Nat. Bu. of Std., V 34, Feb. 1945, p. 143-161.

3. Thompson, Edward B. Jr. Technical Documentary Report No. FDL-TDR-64-22. "Investigations of Catalytic Reactions for CO_2 Reduction". Parts I - V, 1964 - 67. Published by:

   Air Force Flight Dynamics Laboratory
   Research and Technology Division
   Air Force Systems Command
   Wright-Patterson Air Force Base, Ohio

   On sale to the general public from:

   Office of Technical Services
   Department of Commerce
   Washington, D. C.

4. Chemical Engineers' Handbook, 4th edition, John H. Perry, editor. p. 2-62 McGraw-Hill, 1963.

5. Baum, R. A., Kester, F. L. and Lunde, P. J. "Computerized Analytical Technique for Design and Analysis of a Sabatier Reactor Subsystem", Hamilton Standard report No. SVHSER 5082, (1970), prepared on NASA contract 9-9844. Available through National Technical Service Publications. Document No. 71-26295.

Table I
SUMMARY OF EXPERIMENTAL DATA AFTER PRELIMINARY PROCESSING
3.56 GRAMS CATALYST USED IN 4.15 ML REACTOR
INLET/OUTLET PARTIAL PRESSURES SUM TO INLET/OUTLET TOTAL PRESSURE
SPACE VELOCITY AND PCO2 CONSUMED CALCULATED AT REACTOR TEMP AND PRESSURE
INLET FLOW (CUBIC FT/HR) MEASURED AT 19 PSIA AND 73 DEG F
CATALYST COEFFICIENT = 0.25

TEST NUMBER	ABSCISSA X(NP) (1/DEG R)	ORDINATE Y(NP)	REACTOR TEMP. (DEG F)	WALL TEMP (DEG F)	PCO2 CONSUMED (ATM/HR)	SPACE VELOCITY (1/HR)	INLET FLOW (CFH)	INLET CO2 (ATM)	OUTLET CO2 (ATM)	INLET H2 (ATM)	OUTLET H2 (ATM)	INLET H2O (ATM)	OUTLET H2O (ATM)	INLET CH4 (ATM)	OUTLET CH4 (ATM)
519.00	0.001157	3.4184	404.	404.	16.380	1520.	0.2117	0.2036	0.2002	0.8033	0.7984	0.0	0.0115	0.0	0.0058
520.00	0.001120	4.1264	433.	433.	32.730	1548.	0.2117	0.1978	0.1911	0.8091	0.7828	0.0	0.0220	0.0	0.0110
520.10	0.001120	4.0221	433.	433.	29.810	2877.	0.4172	0.2047	0.2015	0.8022	0.7893	0.0	0.0107	0.0	0.0054
521.00	0.001107	4.2811	443.	443.	38.510	2878.	0.4169	0.2036	0.1993	0.8035	0.7870	0.0	0.0137	0.0	0.0069
521.10	0.001085	5.1155	462.	462.	86.250	3874.	0.4172	0.1386	0.1305	0.8683	0.8427	0.0	0.0225	0.0	0.0112
521.40	0.001076	4.8554	469.	469.	67.830	3058.	0.4239	0.2036	0.1970	0.8034	0.7767	0.0	0.0222	0.0	0.0111
522.30	0.001036	5.6127	505.	505.	141.000	3021.	0.4243	0.2055	0.1899	0.8050	0.7422	0.0	0.0453	0.0	0.0226
523.30	0.001042	5.5439	500.	500.	105.500	2792.	0.4256	0.1714	0.1575	0.6814	0.6257	0.1060	0.1444	0.0517	0.0714
524.00	0.001013	5.7263	527.	520.	127.400	2703.	0.4231	0.1790	0.1645	0.6818	0.6224	0.0987	0.1480	0.0475	0.0721
526.00	0.000986	6.2092	552.	543.	199.600	2670.	0.4231	0.1799	0.1573	0.6826	0.5846	0.0968	0.1739	0.0476	0.0861
525.10	0.000995	6.0728	545.	537.	175.500	2671.	0.4231	0.1799	0.1600	0.6800	0.5979	0.0994	0.1575	0.0475	0.0816
526.00	0.000987	5.9528	553.	548.	115.200	2415.	0.4231	0.1487	0.1331	0.5370	0.4721	0.2141	0.2578	0.1071	0.1349
527.00	0.000965	6.3181	576.	567.	157.000	2379.	0.4231	0.1485	0.1272	0.5298	0.4459	0.2197	0.2932	0.1098	0.1457
527.10	0.000981	6.0471	559.	551.	123.500	2393.	0.4231	0.1485	0.1316	0.5298	0.4595	0.2197	0.2778	0.1098	0.1389
527.20	0.000972	6.2076	569.	560.	142.500	2385.	0.4231	0.1485	0.1291	0.5298	0.4490	0.2197	0.2865	0.1098	0.1424
528.10	0.000943	6.7065	600.	587.	218.200	2355.	0.4227	0.1477	0.1181	0.5305	0.4071	0.2197	0.3217	0.1098	0.1600
529.20	0.000945	6.7426	598.	589.	171.000	2228.	0.4223	0.1243	0.0984	0.4362	0.3280	0.2965	0.3859	0.1499	0.1946
530.00	0.000923	7.1121	623.	612.	222.800	2187.	0.4223	0.1255	0.0916	0.4299	0.2878	0.3004	0.4178	0.1510	0.2097
531.00	0.000894	7.3970	652.	634.	252.600	2166.	0.4223	0.1229	0.0846	0.4202	0.2568	0.3059	0.4380	0.1579	0.2245
532.00	0.000899	7.4385	652.	648.	64.010	1928.	0.4223	0.0714	0.0594	0.1805	0.1298	0.5023	0.5441	0.2526	0.2735
533.00	0.000880	7.7548	677.	670.	66.850	1927.	0.4223	0.0714	0.0592	0.1805	0.1287	0.5023	0.5450	0.2526	0.2740
534.00	0.000862	8.2982	700.	694.	73.170	1925.	0.4223	0.0714	0.0582	0.1805	0.1248	0.5023	0.5482	0.2526	0.2755
536.50	0.001163	3.4021	400.	400.	14.520	2836.	0.4352	0.3893	0.3874	0.6175	0.6078	0.0	0.0055	0.0	0.0027
539.50	0.001133	3.9847	423.	423.	26.910	2582.	0.4063	0.3414	0.3374	0.6654	0.6463	0.0	0.0119	0.0	0.0054
540.10	0.001124	4.1673	430.	430.	29.730	2567.	0.4063	0.3435	0.3393	0.6633	0.6427	0.0	0.0120	0.0	0.0060
540.20	0.001111	4.2998	440.	440.	36.660	2564.	0.4063	0.3435	0.3388	0.6633	0.6362	0.0	0.0147	0.0	0.0073
540.80	0.001094	4.5448	450.	450.	46.630	2559.	0.4063	0.3435	0.3382	0.6633	0.6340	0.0	0.0185	0.0	0.0093
541.10	0.001086	5.1762	485.	480.	86.020	2527.	0.4063	0.3455	0.3379	0.6613	0.6117	0.0	0.0336	0.0	0.0168
541.12	0.001086	5.1868	485.	486.	85.250	2528.	0.4063	0.3455	0.3380	0.6613	0.6121	0.0	0.0333	0.0	0.0166
542.00	0.001093	5.1734	490.	485.	85.980	2555.	0.4070	0.3434	0.3359	0.6634	0.6164	0.0	0.0330	0.0	0.0165
542.10	0.001036	5.5506	505.	498.	123.300	2536.	0.4070	0.3434	0.3336	0.6634	0.5955	0.0	0.0472	0.0	0.0236
543.00	0.001047	5.4149	495.	491.	55.830	2284.	0.4070	0.3305	0.3264	0.5117	0.4782	0.1051	0.1314	0.0595	0.0728
544.00	0.001029	5.5951	512.	505.	96.920	2263.	0.4070	0.3312	0.3241	0.5124	0.4567	0.1081	0.1539	0.0552	0.0781
544.10	0.001020	5.6702	520.	514.	103.900	2260.	0.4070	0.3312	0.3236	0.5124	0.4486	0.1081	0.1570	0.0552	0.0797
544.20	0.001012	6.0089	526.	521.	141.600	2243.	0.4070	0.3312	0.3208	0.5124	0.4221	0.1081	0.1752	0.0552	0.0888
544.30	0.001006	6.0740	534.	525.	150.100	2240.	0.4070	0.3312	0.3202	0.5124	0.4170	0.1081	0.1790	0.0552	0.0907
545.00	0.001021	5.6147	519.	512.	85.050	2151.	0.4070	0.3302	0.3226	0.4476	0.3872	0.1543	0.1973	0.0782	0.0997
545.10	0.001012	5.7134	528.	519.	93.110	2153.	0.4073	0.3302	0.3220	0.4476	0.3822	0.1543	0.2010	0.0782	0.1016
545.30	0.001006	5.8705	534.	524.	107.400	2141.	0.4070	0.3302	0.3209	0.4476	0.3722	0.1543	0.2085	0.0782	0.1053
546.10	0.000994	6.1206	541.	532.	121.500	2145.	0.4078	0.3276	0.3192	0.4427	0.3593	0.1547	0.2256	0.0779	0.1138
547.00	0.000969	6.5732	572.	558.	194.800	2106.	0.4070	0.3275	0.3125	0.4428	0.3086	0.1583	0.2578	0.0783	0.1280
548.00	0.000968	6.6161	566.	555.	56.320	1884.	0.4070	0.2847	0.2581	0.1527	0.1021	0.3941	0.4320	0.2624	0.2215
549.00	0.000955	6.7452	587.	581.	69.570	1879.	0.4070	0.2847	0.2568	0.1526	0.0914	0.3941	0.4450	0.2624	0.2255
549.10	0.000952	6.9998	596.	581.	133.500	1929.	0.4070	0.2865	0.2729	0.2477	0.1379	0.3164	0.3984	0.1632	0.2745
550.00	0.000929	7.3386	616.	604.	167.500	1922.	0.4070	0.2855	0.2686	0.2502	0.1146	0.3154	0.4147	0.1627	0.2137
551.00	0.000969	7.6399	640.	628.	196.530	1907.	0.4066	0.2855	0.2659	0.2494	0.0918	0.3161	0.4342	0.1637	0.2221
566.00	0.000923	7.4629	624.	589.	629.500	2327.	0.4067	0.3417	0.2998	0.6886	0.3220	0.0	0.2580	0.0	0.1295
561.00	0.000935	7.2606	610.	568.	363.230	2110.	0.4067	0.3237	0.2943	0.6848	0.2412	0.1375	0.3184	0.0683	0.1563
562.00	0.000942	7.1130	602.	583.	270.100	2045.	0.4059	0.3151	0.2923	0.6143	0.2214	0.1885	0.3322	0.0944	0.1564
563.00	0.000947	7.0040	596.	581.	210.000	1998.	0.4059	0.3017	0.2824	0.5468	0.1880	0.2400	0.3587	0.1217	0.1513
564.00	0.000954	7.0504	598.	578.	131.100	1914.	0.4059	0.2855	0.2721	0.2362	0.1768	0.3214	0.4031	0.1638	0.2248
565.00	0.000954	6.8468	586.	579.	131.900	2004.	0.4321	0.1708	0.1509	0.3028	0.2014	0.3542	0.4340	0.1803	0.2304
566.00	0.000950	7.1900	593.	579.	215.200	1987.	0.4321	0.1960	0.1654	0.3599	0.1984	0.3248	0.4456	0.1274	0.1894
567.00	0.000965	6.9837	594.	580.	277.800	2183.	0.4321	0.2143	0.1800	0.4990	0.3213	0.1981	0.3372	0.0988	0.1684
568.00	0.000944	7.0345	601.	586.	346.000	2269.	0.4321	0.2258	0.1860	0.5672	0.3622	0.1456	0.3264	0.0717	0.1521
569.00	0.000929	7.3290	617.	583.	618.700	2508.	0.4321	0.2600	0.2027	0.7482	0.4515	0.0	0.2361	0.0	0.1175
570.00	0.001009	6.0000	531.	520.	201.900	2632.	0.4311	0.2623	0.2436	0.7514	0.4561	0.0	0.2737	0.0	0.1368
571.00	0.001013	5.8610	527.	520.	122.000	2317.	0.4311	0.2226	0.2078	0.5567	0.4820	0.1567	0.2162	0.0775	0.1063
572.00	0.001014	5.8642	526.	519.	88.950	2301.	0.4311	0.2011	0.1887	0.5043	0.4459	0.2052	0.2479	0.1031	0.1244
573.00	0.001021	5.7880	519.	520.	80.190	2139.	0.4311	0.1924	0.1807	0.4154	0.3571	0.2642	0.3136	0.1367	0.1589
574.00	0.001016	6.3864	524.	520.	167.300	2037.	0.4311	0.1755	0.1584	0.3404	0.2555	0.3308	0.4965	0.1470	0.1999
575.00	0.001016	5.7722	524.	520.	46.150	1978.	0.4311	0.1604	0.1523	0.2654	0.2283	0.3895	0.4196	0.1944	0.2131
576.00	0.001013	5.9192	527.	520.	62.320	2026.	0.4082	0.2828	0.2755	0.2692	0.2176	0.3063	0.3430	0.1554	0.1738
577.00	0.001012	5.7083	528.	520.	73.800	2133.	0.4082	0.3000	0.2923	0.3700	0.3153	0.2288	0.2491	0.1146	0.1345
578.00	0.001011	5.7293	529.	520.	90.350	2211.	0.4082	0.3089	0.3033	0.4350	0.3728	0.1806	0.2255	0.0902	0.1116
579.00	0.001011	5.9664	529.	521.	144.500	2352.	0.4082	0.3223	0.3106	0.5442	0.4566	0.0943	0.1634	0.0474	0.0798
580.00	0.001010	5.8392	530.	520.	151.030	2501.	0.4082	0.3306	0.3195	0.6270	0.5453	0.0386	0.0943	0.0175	0.0473
581.00	0.001009	5.9603	531.	520.	186.600	2620.	0.4558	0.3377	0.3253	0.6760	0.5837	0.0	0.0675	0.0	0.0337
590.00	0.001117	4.5419	435.	0.	49.620	3067.	0.4267	0.1954	0.1849	0.8115	0.7860	0.0	0.0167	0.0	0.0084
591.00	0.001070	5.1849	475.	470.	93.130	3047.	0.4257	0.1954	0.1847	0.8115	0.7668	0.0	0.0304	0.0	0.0152

TABLE II

ACTIVATION ENERGY FROM SERIES 500 TESTS—8/18/70—CO2:.25 H2:1.0—NEW CALIB. CURVES

TEST NUMBER	ABSCISSA X(NP) (1/DEG R)	ORDINATE Y(NP)	REACTOR TEMP. (DEG F)	PCO2 CONSUMED (ATM/HR)	SPACE VELOCITY (1/HR)	INLET CO2 (ATM)	OUTLET CO2 (ATM)	INLET H2 (ATM)	OUTLET H2 (ATM)	INLET H2O (ATM)	OUTLET H2O (ATM)	INLET CH4 (ATM)	OUTLET CH4 (ATM)
519.00	.001120	4.1264	433.	32.730	1946.	.1078	.1911	.8091	.7828	.0000	.0220	.0000	.0110
520.10	.001120	4.0221	433.	29.810	2877.	.2047	.2015	.8022	.7893	.0000	.0107	.0000	.0054
521.00	.001107	4.2811	443.	38.510	2878.	.2034	.1993	.8035	.7870	.0000	.0137	.0000	.0069
521.10	.001085	5.1155	462.	64.250	3874.	.1586	.1305	.8683	.8427	.0000	.0225	.0000	.0112
521.40	.001076	4.8554	469.	67.830	3050.	.2036	.1970	.8034	.7767	.0000	.0222	.0000	.0111
522.30	.001036	5.6127	505.	141.000	3021.	.2053	.1899	.8050	.7422	.0000	.0453	.0000	.0226
523.30	.001042	5.5439	500.	105.500	2792.	.1714	.1575	.6814	.6257	.1060	.1454	.0517	.0714
524.00	.001013	5.7263	527.	127.400	2703.	.1790	.1645	.6818	.6224	.0987	.1480	.0475	.0721
525.00	.000984	6.2092	552.	199.600	2670.	.1799	.1573	.6826	.5896	.0968	.1739	.0476	.0841
525.10	.000995	6.0728	545.	175.300	2671.	.1799	.1600	.6800	.5979	.0994	.1675	.0476	.0816
526.00	.000987	5.9528	553.	115.200	2415.	.1687	.1331	.5370	.4721	.2141	.2678	.1071	.1340
527.00	.000965	6.3181	576.	157.600	2379.	.1685	.1272	.5298	.4409	.2197	.2932	.1090	.1457
527.10	.000981	6.0471	559.	123.500	2393.	.1685	.1316	.5298	.4595	.2197	.2778	.1090	.1380
527.20	.000972	6.2076	569.	142.500	2385.	.1685	.1291	.5298	.4490	.2197	.2865	.1090	.1424
528.10	.000943	6.7065	600.	218.200	2355.	.1677	.1181	.5305	.4071	.2197	.3217	.1090	.1600
529.20	.000945	6.7420	598.	171.800	2228.	.1403	.0984	.4362	.3280	.2965	.3859	.1499	.1946
530.00	.000923	7.1121	623.	222.800	2187.	.1255	.0916	.4299	.2878	.3004	.4170	.1510	.2097
531.00	.000899	7.3570	652.	252.400	2166.	.1229	.0846	.4202	.2590	.3059	.4340	.1579	.2245
532.00	.000890	7.4185	652.	64.010	1928.	.0714	.0594	.1805	.1290	.5023	.5441	.2526	.2735
533.00	.000880	7.7548	677.	66.650	1927.	.0714	.0592	.1805	.1287	.5023	.5450	.2526	.2740
534.00	.000862	8.2982	700.	73.170	1925.	.0714	.0582	.1805	.1248	.5023	.5482	.2526	.2756
538.50	.001163	3.4021	400.	14.820	2836.	.3493	.3474	.6175	.6078	.0000	.0055	.0000	.0027
539.50	.001133	3.9848	423.	26.910	2562.	.3414	.3374	.6654	.6463	.0000	.0109	.0000	.0054
540.10	.001126	4.0873	430.	29.730	2567.	.3435	.3393	.6633	.6427	.0000	.0120	.0000	.0060
540.20	.001111	4.2998	440.	30.660	2564.	.3435	.3388	.6633	.6392	.0000	.0147	.0000	.0073
540.80	.001099	4.5448	450.	46.430	2589.	.3435	.3382	.6633	.6340	.0000	.0165	.0000	.0093
541.10	.001058	5.1762	485.	86.020	2527.	.3455	.3379	.6613	.6117	.0000	.0336	.0000	.0168
541.12	.001056	5.1068	485.	85.250	2528.	.3455	.3380	.6613	.6121	.0000	.0333	.0000	.0166
542.00	.001053	5.1734	490.	85.980	2555.	.3434	.3359	.6634	.6146	.0000	.0330	.0000	.0165
542.10	.001034	5.5506	505.	123.300	2538.	.3434	.3336	.6634	.5955	.0000	.0472	.0000	.0236
543.00	.001047	5.8149	495.	55.430	2284.	.3305	.3264	.5117	.4762	.1051	.1314	.0595	.0720
544.00	.001029	5.5951	512.	96.920	2263.	.3312	.3241	.5124	.4507	.1081	.1539	.0552	.0781
544.10	.001020	5.6708	520.	163.500	2260.	.3312	.3236	.5124	.4466	.1081	.1570	.0552	.0797
544.20	.001012	6.0089	528.	141.400	2243.	.3312	.3208	.5124	.4221	.1081	.1752	.0552	.0888
544.30	.001006	6.0746	534.	150.100	2240.	.3312	.3202	.5124	.4170	.1081	.1790	.0552	.0907
545.00	.001021	5.6147	519.	85.050	2151.	.3302	.3226	.4476	.3872	.1543	.1973	.0782	.0997
545.10	.001012	5.7134	520.	93.110	2153.	.3302	.3220	.4476	.3822	.1543	.2010	.0782	.1016
545.30	.001006	5.8705	534.	107.400	2141.	.3302	.3209	.4476	.3722	.1543	.2085	.0782	.1053
546.10	.000999	6.0206	541.	121.500	2145.	.3276	.3182	.4427	.3503	.1587	.2206	.0779	.1088
547.00	.000969	6.5732	572.	194.800	2106.	.3275	.3125	.4428	.3086	.1583	.2578	.0783	.1280
548.00	.000966	6.6161	568.	56.320	1884.	.2647	.2581	.1527	.1021	.3941	.4320	.2024	.2215
549.00	.000956	6.9452	587.	69.570	1879.	.2647	.2568	.1528	.0914	.3941	.4400	.2024	.2255
549.10	.000952	6.9996	590.	133.500	1929.	.2665	.2729	.2477	.1379	.3164	.3984	.1632	.2045
550.00	.000929	7.3386	616.	167.500	1922.	.2655	.2686	.2582	.1146	.3154	.4167	.1627	.2137
551.00	.000909	7.6599	640.	196.500	1987.	.2655	.2659	.2494	.0916	.3161	.4342	.1627	.2221

EQUATION FOR ACTIVATION ENERGY IS
LOG(RATE/(C-O)) = LOG(K) - (EACT/RT), WHERE (C-O) = F(PCO2, PH2, PH2O, PCH4, KEQ)

ACT. ENERGY = .30593+05 AND INTERCEPT = .2141+02

TABLE III

RATE CONSTANT FROM SERIES 500 TESTS—8/20/70—CO2:.25 H2:1.0—NEW CALIB. CURVES. DATE 08/20/70 TIME 1

FORWARD RATE CONSTANT OF SABATIER REACTION BY RUNGE-KUTTA INTEGRATION

TEST NUMBER	RATE CONSTANT (1/HR-ATM)	REACTOR TEMP. (DEG F)	SPACE VELOCITY (1/HR)	ACTIVATION ENERGY (BTU/LB-MOLE CO2)	PCO2 CONSUMED (ATM)	INLET CO2 (ATM)	INLET H2 (ATM)
519.0	.17866+10	444.	1940.	30593.	.0187	.2034	.8033
520.0	.00130+10	433.	1940.	30593.	.0211	.1978	.8091
520.1	.17787+10	433.	2877.	30593.	.0186	.2047	.8022
521.0	.19189+10	443.	2878.	30593.	.0186	.2034	.8035
521.1	.31796+10	462.	3874.	30593.	.0273	.1386	.8683
521.4	.21830+10	469.	3048.	30593.	.0272	.2036	.8034
522.3	.86307+10	505.	3021.	30593.	.0467	.2055	.8050
523.3	.26801+10	500.	2792.	30593.	.0370	.1714	.6814
524.0	.21384+10	527.	2703.	30593.	.0472	.1790	.6818
525.0	.36663+10	552.	2670.	30593.	.0798	.1799	.6826
525.1	.26727+10	545.	2671.	30593.	.0659	.1799	.6800
526.0	.18876+10	553.	2415.	30593.	.0479	.1687	.5370
527.0	.22828+10	576.	2379.	30593.	.0661	.1685	.5298
527.1	.19818+10	559.	2393.	30593.	.0516	.1685	.5298
527.2	.20762+10	569.	2385.	30593.	.0597	.1685	.5298
528.1	.31250+10	600.	2355.	30593.	.0908	.1677	.5305
538.5	.17802+10	400.	2836.	30593.	.0050	.3493	.6175
539.5	.20640+10	423.	2562.	30593.	.0108	.3414	.6654
540.1	.20083+10	430.	2567.	30593.	.0116	.3435	.6633
540.2	.20606+10	440.	2564.	30593.	.0143	.3435	.6633
540.8	.22006+10	450.	2589.	30593.	.0188	.3435	.6633
541.1	.23220+10	485.	2527.	30593.	.0341	.3455	.6613
541.1	.22910+10	485.	2528.	30593.	.0337	.3455	.6613
542.0	.21820+10	490.	2555.	30593.	.0337	.3434	.6634
542.1	.25358+10	505.	2538.	30593.	.0486	.3434	.6634
543.0	.16463+10	495.	2284.	30593.	.0294	.3305	.5117
544.0	.23876+10	512.	2263.	30593.	.0427	.3312	.5124
544.1	.23070+10	520.	2260.	30593.	.0448	.3312	.5124
544.2	.31835+10	528.	2243.	30593.	.0631	.3312	.5124
544.3	.31272+10	534.	2240.	30593.	.0671	.3312	.5124
545.0	.21980+10	519.	2151.	30593.	.0396	.3302	.4476
545.1	.21912+10	520.	2153.	30593.	.0432	.3302	.4476
545.3	.23045+10	534.	2141.	30593.	.0588	.3302	.4476
546.1	.26120+10	541.	2145.	30593.	.0646	.3276	.4427
570.0	.28758+10	531.	2632.	30593.	.0788	.2823	.7514
571.0	.25637+10	527.	2317.	30593.	.0578	.2826	.5567
572.0	.19815+10	526.	2361.	30593.	.0370	.2811	.5063
573.0	.20461+10	519.	2199.	30593.	.0375	.1994	.4152
575.0	.23087+10	526.	1974.	30593.	.0834	.1600	.7054
576.0	.27775+10	527.	2036.	30593.	.0307	.2828	.2697
577.0	.28706+10	528.	2133.	30593.	.0381	.4000	.3700
578.0	.21363+10	520.	2211.	30593.	.0600	.4000	.0300
579.0	.28678+10	529.	2342.	30593.	.0615	.4273	.4462
580.0	.23000+10	530.	2561.	30593.	.0606	.3306	.4279
581.0	.27156+10	531.	2626.	30593.	.0786	.3377	.4760

STANDARD DEVIATION OF ABOVE RATE CONSTANTS = .5007+09

TABLE IV - Selection of Experimental Data

Selection of runs for activation energy determination
(Table II, Figures 7 and 8)

		Reason
Planned:	Runs 519 - 551	
Dropped:	Run 519	Reaction rate so low that analyses were in doubt
Used:	Runs 520 - 551	

Selection of runs for rate constant determination
(Table III)

Planned:	Runs 560 - 581	
Dropped:	Runs 560 - 569 (entire 580° bath temperature series)	High difference between wall and reactor temperatures due to generally high conversions caused doubt as to actual reaction temperature.
Added:	Runs 519 - 528.1 538.5 - 546.1	Lower temperature runs from activation energy series replaced above data.
Used:	Runs 519 - 528.1 538.5-546.1 570 - 581	

Runs 590 and 591 were extra runs not planned and not used.

FIGURE 1 THERMODYNAMIC EQUILIBRIA FOR THE SABATIER REACTION

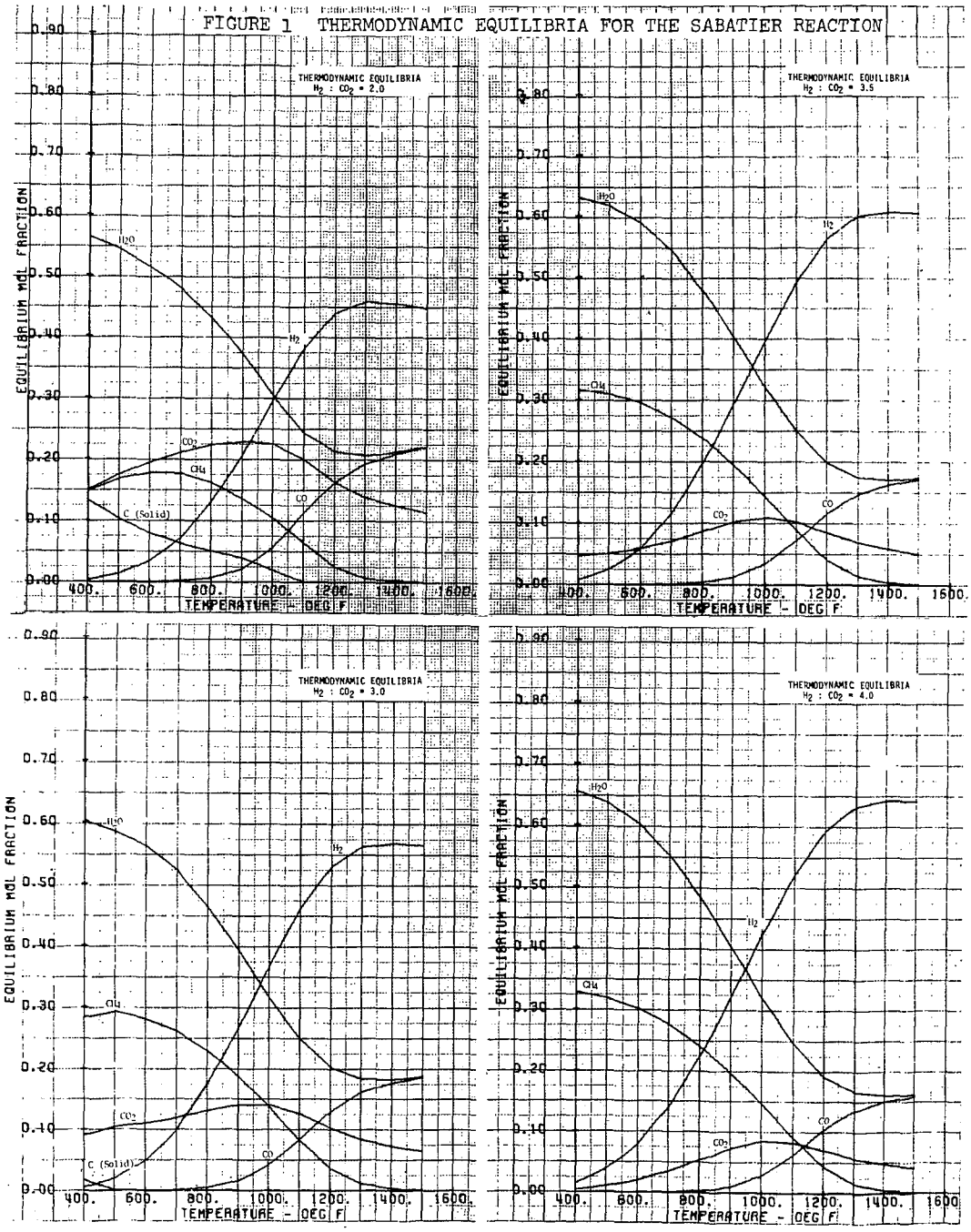

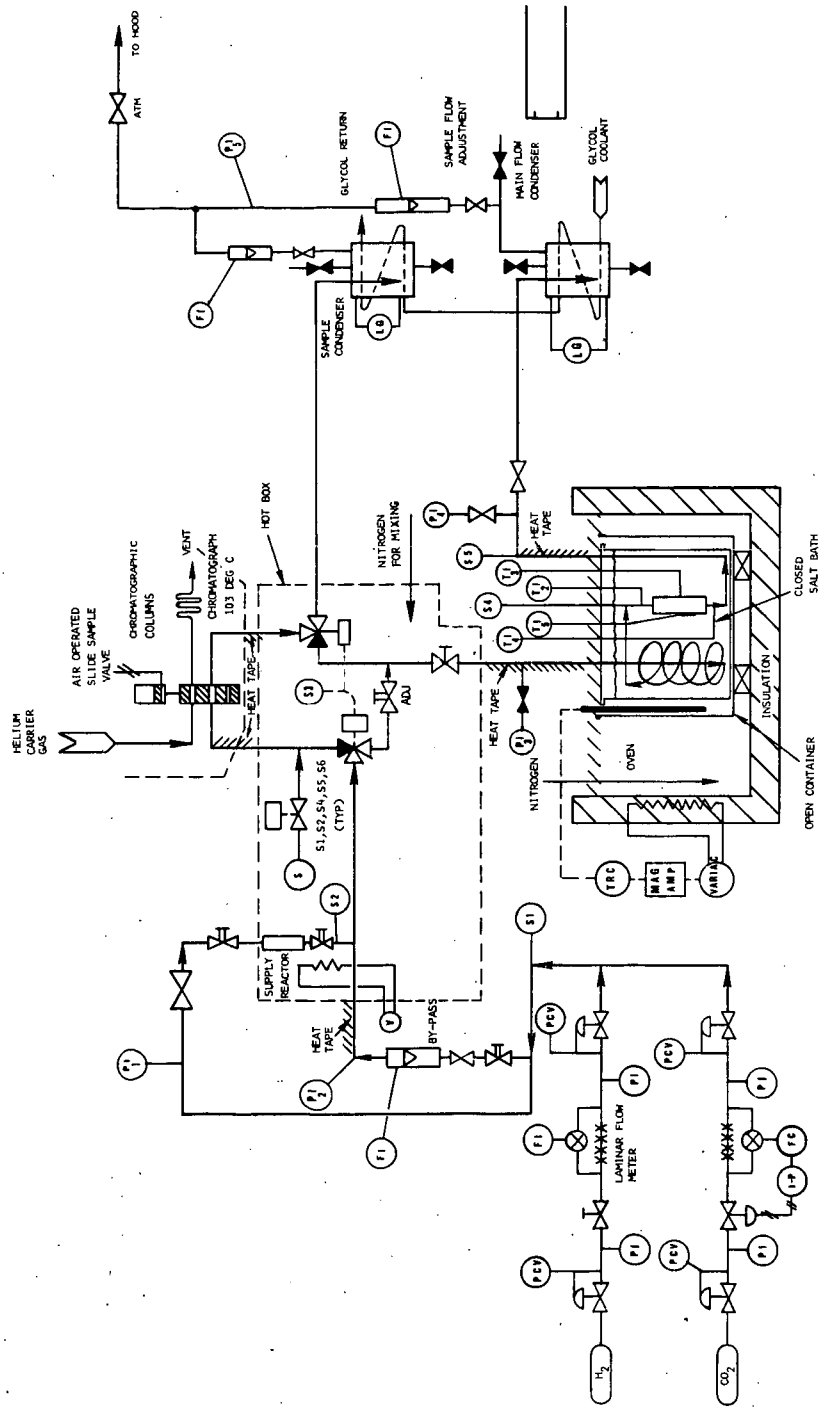

FIGURE 2. RATE DATA APPARATUS, SABATIER REACTION

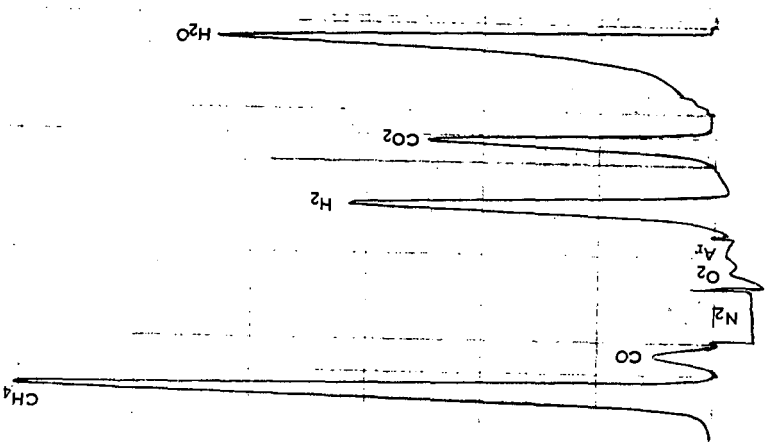

FIGURE 4 CHROMATOGRAPHIC TRACE

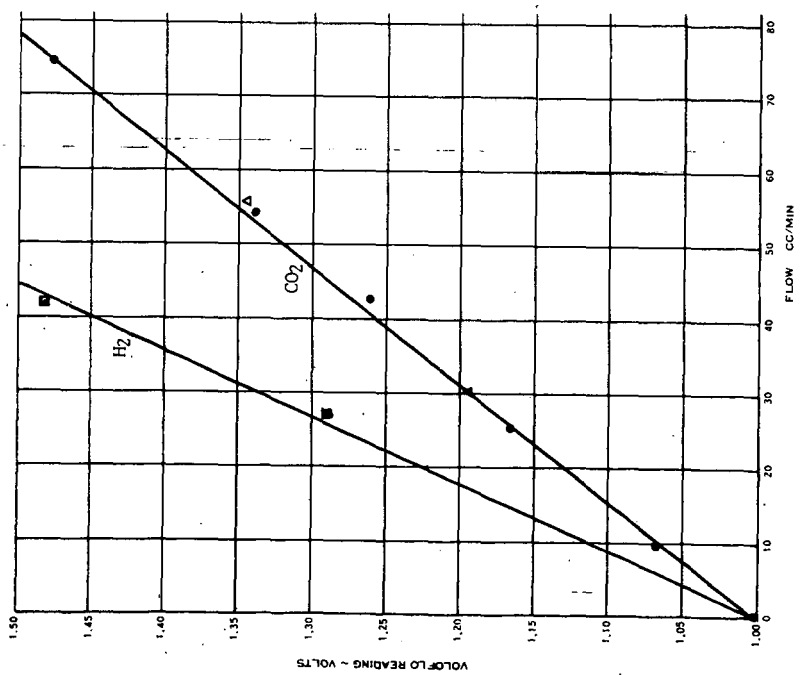

FIGURE 3 VOLOFLO CALIBRATION CURVE FOR CO_2 AND H_2

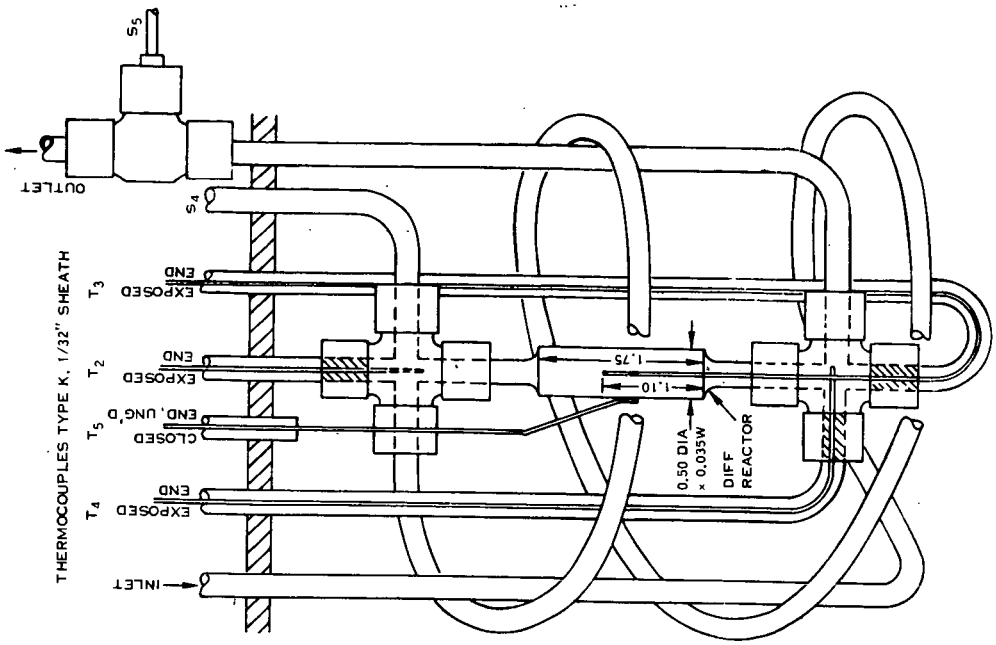

FIGURE 6 TEST REACTOR SABATIER

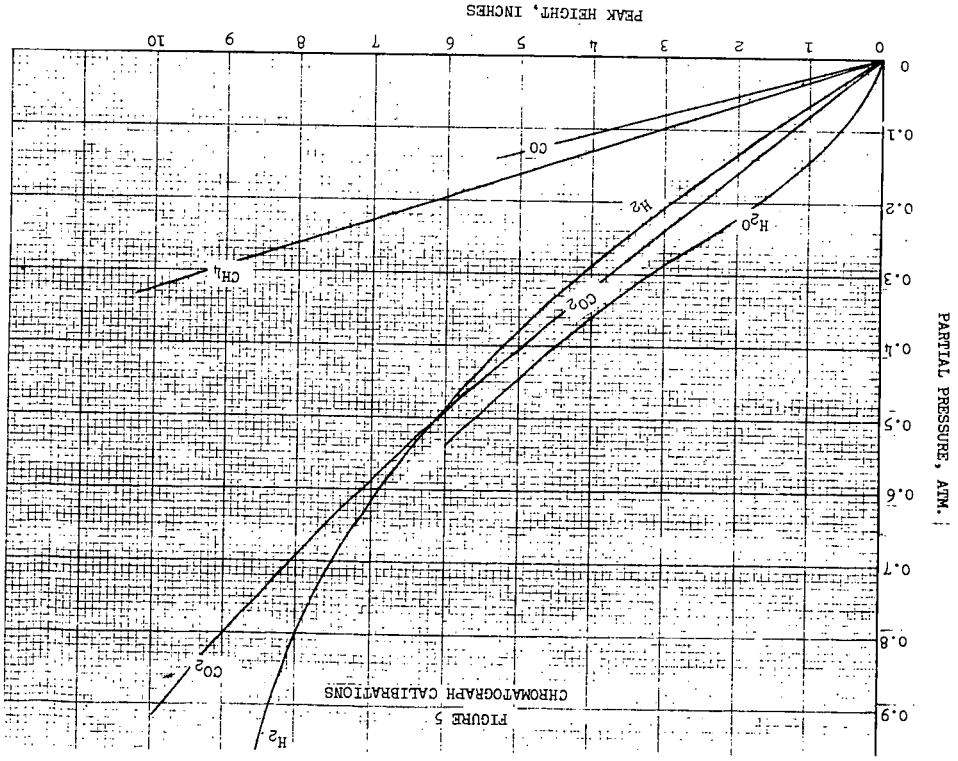

FIGURE 5
CHROMATOGRAPH CALIBRATIONS

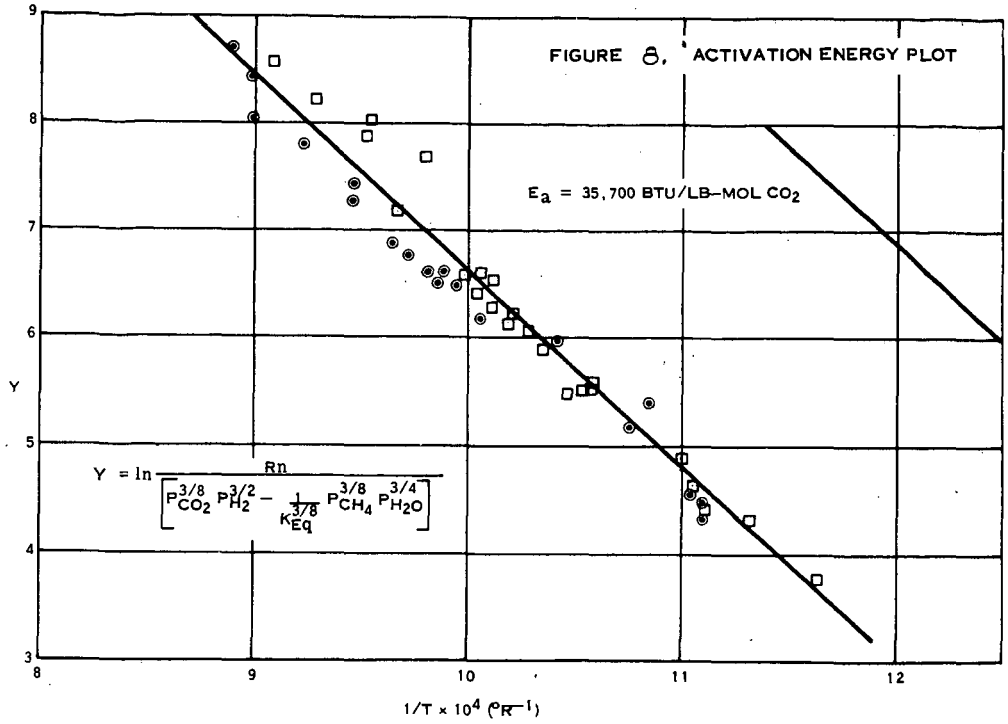
FIGURE 8. ACTIVATION ENERGY PLOT
E_a = 35,700 BTU/LB-MOL CO_2
$Y = \ln \frac{Rn}{\left[P_{CO_2}^{3/8} P_{H_2}^{3/2} - \frac{1}{K_{Eq}^{3/8}} P_{CH_4}^{3/8} P_{H_2O}^{3/4}\right]}$
Y
$1/T \times 10^4$ (°R^{-1})

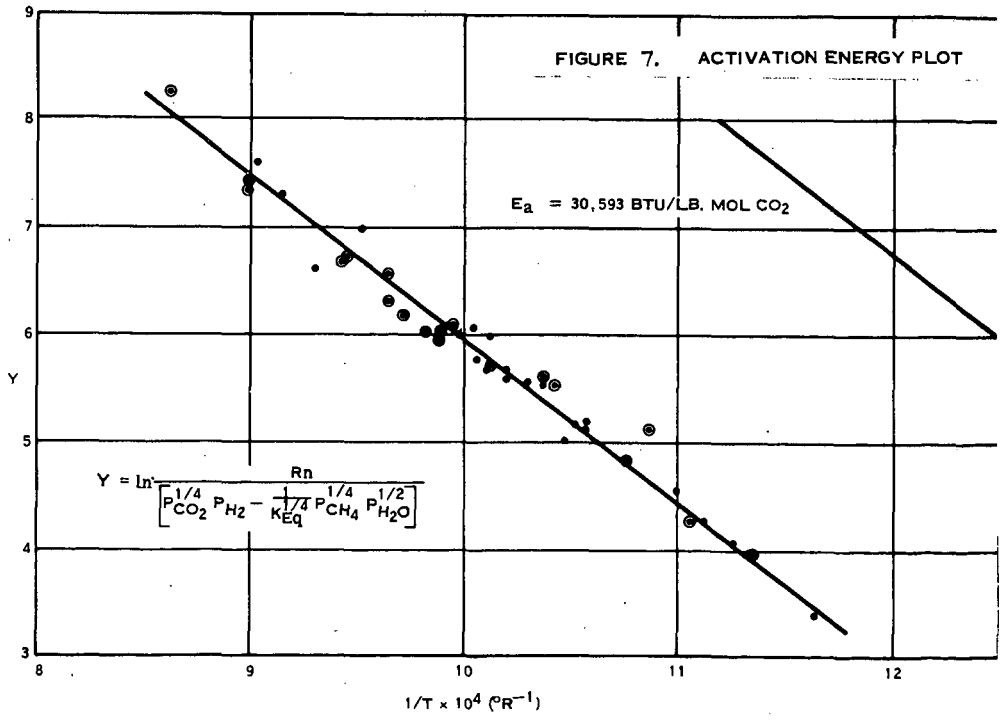
FIGURE 7. ACTIVATION ENERGY PLOT
E_a = 30,593 BTU/LB. MOL CO_2
$Y = \ln \frac{Rn}{\left[P_{CO_2}^{1/4} P_{H_2} - \frac{1}{K_{Eq}^{1/4}} P_{CH_4}^{1/4} P_{H_2O}^{1/2}\right]}$
Y
$1/T \times 10^4$ (°R^{-1})

28

Coal Hydrogenation in Small Tube Reactors

R. E. Wood and G. R. Hill

Department of Mining, Metallurgy and Fuels Engineering
University of Utah
Salt Lake City, Utah

The office of Coal Research short residence time coal hydrogenation reactor at the University of Utah has been previously discussed in Hydrocarbon Processing[1] and The Quarterly of the Colorado School of Mines[2].

A schematic diagram of this device is shown in Figure 1. It contains provision for passing dry powdered coal through a heated and pressurized reaction zone. The reactor is mounted vertically and the coal is pushed by means of an auger feeder into the top and the reaction products are collected in a water cooled quench tank at the bottom. This reactor can be pressurized to 5000 PSI and heated to 800°C.

Although conversions to 75 or 80 percent of the coal matter can be realized in this apparatus, it suffers from some rather crippling deficiencies. Of greatest importance in limiting the usefulness of the device is the fact that coal, in falling through the reaction zone becomes plastic and sticky. Some of the liquid-solid product sticks to the reactor walls, becomes devolitilized and the residue remains as a solid char that builds up to eventually block the passage. A second factor is that the limited capacity of the compressor (240 cubic feet per hour maximum) severely restricts the movement of gas through the reaction zone. This essentially stagnant reactor space contributes to the coal and char sticking problem as there is little flow of gas to force the solid material through to the quench vessel.

Calculations of Reynolds numbers for hydrogen at 2000 PSI and 700°C reveals that a flow of 200 cubic feet perhour will not provide turbulent flow in tubes larger than 3/16 inch I.D. Therefore, we restricted the reactor tube size to 1/8 inch and proceeded to work with hydrogen-coal slurries in this type of reactor.

The auger feeder used with the 2 inch I.D. reactor is not adaptable to the 1/8 inch tube because it delivers coal in slugs rather than at a steady rate. The small tube is blocked by each slug of coal delivered by the auger. For this reason a fluidized feeder, where hydrogen gas passing through a coal bed carries the coal into the small tube reactor was developed. The design of this feeder, with the small tube reactor is indicated in Figure 3. This schematic shows the 1/8 inch tube mounted inside the 2 inch tube of the original reactor. This construction adds a further factor in that heat to raise the coal to reaction temperature must be added from outside the 2 inch reactor. Convection and radiation from the inner wall of the larger reactor is insufficient to heat the small tube enough to permit it in turn to properly heat the coal-hydrogen stream passing through it. Therefore, a chamber was constructed around the inner tube such that a molten lead bath could be used to transmit heat from the walls of the outer tube to the inner reactor.

Figure 4 shows the product distribution, in terms of gases and liquids, produced as a function of temperature and pressure for one of the more reactive coal types. This is Orangeville, Utah, coal, a high-volatile bituminous "B" coal from East Central Utah. The production of gases, primarily Methane but with substantial quantities of ethane, propane and higher carbon number hydrocarbon gases; and liquids, a very complicated mixture of aliphatic and aromatic materials is shown at four temperatures and three pressures. Increasing temperature increases the output of both gases and liquids, but the liquids are increased to a greater extent. Increased pressure likewise increases the production of liquids. Above 2000 PSI the gas production is decreased to some extent. The total conversion, equal to the sum of gases

plus liquids is over 60 percent of the original coal material at 675°C and 2000 PSI.

Table I is a compilation of data obtained on several different coals in this small tube reactor. Since these samples were measured over a period of several months, the reaction conditions were not completely uniform. Most were obtained at 1750 PSI hydrogen pressure and 650°C temperature, but some were measured at 675°C and 2000 PSI. The conditions were selected at less than a maximum conversion operation in an effort to spread the data to show coal differences. We have listed the coal, total conversion, feed rate, oxygen content and some observations about the coal. The coals are naturally broken into three categories. The first category contains those coals that are easy to feed and give little or no reactor plugging but which also give very little reaction. These are coals with high oxygen content and are generally of the lignite and subbituminous types. The second group of coals have an intermediate reaction, are not really difficult to feed, give some plugging and have an intermediate oxygen content. The third category of coals is generally the high volatile, non-caking bituminous coals that show good reaction without excessive plugging. Feeding with our hopper arrangement is difficult with these coals because they are sticky and agglomerate readily, particularly when the catalyst is present. This third group of coals is the most interesting because they react most readily. The conversions reported on these coals were obtained with half the catalyst application used with the other types. The lack of conversion numbers on some of these coals was because the higher level of catalyst was used and both feeding and plugging problems were encountered.

Table I. Comparison of Coals Treated in 1/8 inch I.D. reaction tube

	Conversion	Feed Rate g/m	% O_2	Coal Characteristic		
				Feeding	Reacting	Plugging
Sidney, Montana (Lignite)	11.1	19	21.0	GOOD	POOR	NONE
Big Horn, Wyoming	10.3	13	11.2	"	"	"
Navajo, Utah	17.5	14	----	"	"	"
Beluga River, Canada	17.9	10	28.3	"	"	"
Kanab, Utah	6.8	11	13.6	"	"	"
Alton, Utah	7.6	18	24.9	"	"	"
River King, Illinois	30.6	8	8.9	FAIR	FAIR	SOME
Last Chance, Utah	37.2	14	18.6	"	"	"
Kaiparowitz, Utah	45.0	--	18.0	"	"	"
Coalville, Utah	38.8	--	10.3	"	"	"
Powers, Utah	37.2	9	----	"	"	"
Geneva-Somerset, Utah-Colo.	48.4	14	6.4	POOR	GOOD	SOME
Spencer, Utah	44.1	9	12.3	"	"	"
Castle Valley, Utah	56.6	8	5.7	"	"	"
Orangeville, Utah	66.5	2	----	"	"	"
Hiawatha, Utah	76.8	8	----	"	"	"
Cedar City, Utah	----	--	7.5	"	"	"
Castle Gate, Utah	----	--	5.5	"	"	"
Coal Basin, Colorado	----	--	3.0	"	"	"
Bear, Colorado	----	--	8.5	"	"	"

Figure 5 shows the effect of changing catalyst concentration on two types of coal. The catalyst was zinc chloride and the application was measured in terms of weight of zinc metal to MAF coal. For Orangeville, Utah, coal, a good reacting material, the doubling of catalyst concentration accomplished little or nothing. For the Kaiparowitz coal, an intermediate reactor by our other standards, more catalyst gives a marked increase in conversion.

The coal feed rate is a process variable that is difficult to control with a fluidized feeder. It is affected by moisture content, concentration of catalyst, particle size and surface character of the coal particles. Figure 6 is an attempt to show the effect of both feed rate and particle size on the conversion in this process. The length of the horizontal lines indicate the mesh size range of the particles sample. The number by the line indicates the feed rate in grams of coal per minute. Two coals were studied. Kaiparowitz as shown in Figure 5 and Castle Gate, Utah, which is one of the better reacting type coals.

In general, we see that an increase in feed rate results in decreased reaction, presumably because of less efficient heating of larger quantities of coal to the required reaction condition. We see also that a decrease in particle size results in a decreased reaction. This is not to be expected because smaller coal particles should be heated more efficiently. The reason for this decreased reaction lies in the actual residence time of the coal within the heated zone. Because of the small size of the reactor, it has not been possible to insert probes, or even thermocouples to measure residence times. However, we have been able to observe pressure buildup and decay as a small amount of coal is injected. We calculate that the gas is flowing at a rate where its residence in the hot zone is in the range of 0.01 to 0.03 seconds. However, the coal is traveling much less rapidly. Actually, it approaches a plug-flow condition. The pressure difference between top and bottom of the reactor tube increases as coal is injected and decays within 5-10 seconds. The coal residence then is somewhere in the range 1 to 10 seconds. This is somewhat dependent on particle size. The smaller particles tend to be carried with the gas and go through in less than 0.1 second. This is not long enough to heat even the finest particles enough to cause reaction. This, then is the reason for decreased reaction with a smaller particle size sample as indicated by the data of Figure 7.

The catalyst used in this work has been primarily $ZnCl_2$. It's action in the coal hydrogenation reaction is not understood although as a Lewis acid it is expected to act as a cracking catalyst for large organic molecules and the hydrogen reacts with the molecular fragments produced. Some studies have been made in an effort to discover the catalytically active form of the zinc and to devise schemes for recovering the zinc from the char for use on fresh coal. The economic success of the process will certainly depend on the almost complete recovery of this material.

Several kinds of inorganic materials have been tested as catalysts for this coal process. Table 2 shows the coal conversion obtained with each of these materials using the same coal and reaction conditions. Zinc halides and stannous chloride are the most effective of those tested. The zinc chloride is by far the cheaper material and therefore is the best selection.

Table 2. Comparison of Inorganic Salt Catalysts

Salt	Percent Conversion	Salt	Percent Conversion
$ZnBr_2$	58.5	Sn(powder)	7.9
ZnI_2	46.3	$CuCl_2.2H_2O$	7.6
$ZnCl_2$	41.1	$FeCl_3.6H_2O$	7.2
$SnCl_2 \cdot 2H_2O$	40.5	Zn(powder)	7.0
$SnCl_4 \cdot 5H_2O$	25.6	$ZnSO_4.7H_2O$	5.4
LiI	16.6	$(NH_4)_6Mo_7O_{24}.4H_2O$	5.4
$CrCl_3$	12.8	$FeCl_2$	3.3
$Pb(C_2H_3O_2)_2.3H_2O$	11.7	$CaCl_2.H_2O$	No Reaction
NH_4Cl	11.0	$Na_2CO_3.H_2O$	No Reaction
$CdCl_2.2\ 1/2\ H_2O$	7.9		

Conditions

Last Chance, Utah, Coal 40-100 mesh — Feed Rate 10-12 g/m
Pressure 1750 PSI — Reactor, 1/8" I.D. Tube
Temperature 650°C — 3 Ft. Heated Section
Catalyst Concentration, 0.06 Weight Metal/Weight Coal (MAF)

Just which form of zinc is catalytically active is not known. We do know that the chloride reacts with aldehydes, ketones and ether oxygen configurations to form complexes. We find that when zinc chloride is impregnated onto coal surfaces, all is not recovered by water extraction. After the coal has been heated even less of the zinc can be extracted by water alone. Table 3 shows the forms of zinc that we have identified in the char product where almost all the zinc is found after reaction. The residual zinc chloride is water soluble but zinc metal, basic zinc chloride and zinc oxide are insoluble in water and require an acid for solution. The basic zinc chloride is formed by reaction with water at elevated temperatures. We have found the zinc metal in char samples and have found zinc oxide in samples subjected to microwave ashing to remove the carbonaceous material. We have not verified the presence of zinc sulfide, but feel that it may be the form of zinc least soluble in hydrochloric acid and therefore a suspect as to the form in which the zinc is most difficultly recoverable.

Table III. Compounds of Zinc in Char

Coal	Char	Solubility
	$ZnCl_2$	H_2O
	Zn	HCl
$ZnCl_2$	$ZnCl_2 \cdot 4Zn(OH)_2$*	HCl
	ZnO**	HCl
	ZnS (not verified)	Slowly soluble in HCl

* Found in H_2O insoluble portion of heated H_2O solution of $ZnCl_2$

** Found in ash from low temperature ashing of char to remove organic matter and carbon.

Figure 7 shows the recovery from reacted char, using hydrochloric and sulfuric acids, 10 percent in each case. The lower designation is the number of times the same sample was extracted with equal portions of fresh hot acid. About half the zinc, as measured by the intensity of the zinc K alpha x-ray fluorescence line, is readily extracted but the remainder is only slowly extracted. It could be a rather long and involved procedure to recover all the zinc by acid extraction alone.

Because of the fact that zinc sulfide is a potential form of the zinc after the reaction we have considered some methods for dissolving this product. Table 4 shows some solution reactions together with the solubility products involved. Dissolving ZnS in HCl is possible by virtue of the formation of slightly ionized H_2S and the volitilization of H_2S from the solution. Dissolving ZnS in solutions of Pb^{++}, Cu^{++} or Hg^{++} ions is possible because these metal ions form sulfides even less soluble than ZnS. Mercury sulfide particularly is very insoluble.

Table IV. Some Reactions for Dissolving ZNS.

$ZnS(solid) + HCl$	$Zn^{++} + 2Cl^- + H_2S$	ZnS	$K_{SP} = 1.2 \times 10^{-23}$ (18°C)
$ZnS(solid) + Pb^{++}$	$Zn^{++} + PbS(solid)$	PbS	$K_{SP} = 3.4 \times 10^{-28}$ (18°C)
$ZnS(solid) + Cu^{++}$	$Zn^{++} + CuS(solid)$	CuS	$K_{SP} = 8.5 \times 10^{-45}$ (18°C)
$ZnS(solid) + Hg^{++}$	$Zn^{++} + HgS(solid)$	HgS	$K_{SP} = 4.0 \times 10^{-53}$ (18°C)

Figure 8 shows the extraction of zinc from reacted coal char, first with hot water, then with hot concentrated hydrochloric acid and then with hot dilute solutions of Pb^{++}, Cu^{++}, and Hg^{++} ions. We notice first that the difficulty of removing zinc from the char is directly related to the amount of conversion. For high conversion less zinc is dissolved by the solvent. Longer exposure to the Hg^{++} ion would probably result in essentially complete recovery. This approach is not practical for actual recovery of zinc, but it does illustrate that the zinc is present in the char in a very insoluble form, probably as the sulfide and that some extreme method will be required to recover the catalyst. Tests have indicated that char can be recycled with fresh coal and catalyst without loss of catalytic character. These tests have further indicated that recycled char by itself can be further hydrogenated. The resulting product is higher in gas and lower in liquids than the first cycle but the percent conversion is near to that in the first case. These tests need further study and verification because the difficulty of feeding char alone makes these tests less reliable than when coal alone is fed.

References

1. Qader, S. A., Haddadin, R. A. Anderson, L. L., Hill, G. R., Hydrocarbon Processing 48, No. 9, 147 (1969).

2. Wood, R. E., Anderson, L. L., and Hill, G. R., Quarterly of the Colorado School of Mines, Vol. 65, No. 4, 201 (1970).

Conditions

Last Chance, Utah, Coal 40-100 mesh — Feed Rate 10-12 g/m
Pressure 1750 PSI — Reactor, 1/8" I.D. Tube
Temperature 650°C — 3 Ft. Heated Section
Catalyst Concentration, 0.06 Weight Metal/Weight Coal (MAF)

Just which form of zinc is catalytically active is not known. We do know that the chloride reacts with aldehydes, ketones and ether oxygen configurations to form complexes. We find that when zinc chloride is impregnated onto coal surfaces, all is not recovered by water extraction. After the coal has been heated even less of the zinc can be extracted by water alone. Table 3 shows the forms of zinc that we have identified in the char product where almost all the zinc is found after reaction. The residual zinc chloride is water soluble but zinc metal, basic zinc chloride and zinc oxide are insoluble in water and require an acid for solution. The basic zinc chloride is formed by reaction with water at elevated temperatures. We have found the zinc metal in char samples and have found zinc oxide in samples subjected to microwave ashing to remove the carbonaceous material. We have not verified the presence of zinc sulfide, but feel that it may be the form of zinc least soluble in hydrochloric acid and therefore a suspect as to the form in which the zinc is most difficultly recoverable.

Table III. Compounds of Zinc in Char

Coal	Char	Solubility
	$ZnCl_2$	H_2O
	Zn	HCl
$ZnCl_2$	$ZnCl_2 \cdot 4Zn(OH)_2$*	HCl
	ZnO**	HCl
	ZnS (not verified)	Slowly soluble in HCl

* Found in H_2O insoluble portion of heated H_2O solution of $ZnCl_2$

** Found in ash from low temperature ashing of char to remove organic matter and carbon.

Figure 7 shows the recovery from reacted char, using hydrochloric and sulfuric acids, 10 percent in each case. The lower designation is the number of times the same sample was extracted with equal portions of fresh hot acid. About half the zinc, as measured by the intensity of the zinc K alpha x-ray fluorescence line, is readily extracted but the remainder is only slowly extracted. It could be a rather long and involved procedure to recover all the zinc by acid extraction alone.

Because of the fact that zinc sulfide is a potential form of the zinc after the reaction we have considered some methods for dissolving this product. Table 4 shows some solution reactions together with the solubility products involved. Dissolving ZnS in HCl is possible by virtue of the formation of slightly ionized H_2S and the volitilization of H_2S from the solution. Dissolving ZnS in solutions of Pb^{++}, Cu^{++} or Hg^{++} ions is possible because these metal ions form sulfides even less soluble than ZnS. Mercury sulfide particularly is very insoluble.

Table IV. Some Reactions for Dissolving ZNS.

$ZnS(solid) + HCl$	$Zn^{++} + 2Cl^- + H_2S$	ZnS	$K_{SP} = 1.2 \times 10^{-23}$ (18°C)
$ZnS(solid) + Pb^{++}$	$Zn^{++} + PbS(solid)$	PbS	$K_{SP} = 3.4 \times 10^{-28}$ (18°C)
$ZnS(solid) + Cu^{++}$	$Zn^{++} + CuS(solid)$	CuS	$K_{SP} = 8.5 \times 10^{-45}$ (18°C)
$ZnS(solid) + Hg^{++}$	$Zn^{++} + HgS(solid)$	HgS	$K_{SP} = 4.0 \times 10^{-53}$ (18°C)

Figure 8 shows the extraction of zinc from reacted coal char, first with hot water, then with hot concentrated hydrochloric acid and then with hot dilute solutions of Pb^{++}, Cu^{++}, and Hg^{++} ions. We notice first that the difficulty of removing zinc from the char is directly related to the amount of conversion. For high conversion less zinc is dissolved by the solvent. Longer exposure to the Hg^{++} ion would probably result in essentially complete recovery. This approach is not practical for actual recovery of zinc, but it does illustrate that the zinc is present in the char in a very insoluble form, probably as the sulfide and that some extreme method will be required to recover the catalyst. Tests have indicated that char can be recycled with fresh coal and catalyst without loss of catalytic character. These tests have further indicated that recycled char by itself can be further hydrogenated. The resulting product is higher in gas and lower in liquids than the first cycle but the percent conversion is near to that in the first case. These tests need further study and verification because the difficulty of feeding char alone makes these tests less reliable than when coal alone is fed.

References

1. Qader, S. A., Haddadin, R. A. Anderson, L. L., Hill, G. R., Hydrocarbon Processing 48, No. 9, 147 (1969).

2. Wood, R. E., Anderson, L. L., and Hill, G. R., Quarterly of the Colorado School of Mines, Vol. 65, No. 4, 201 (1970).

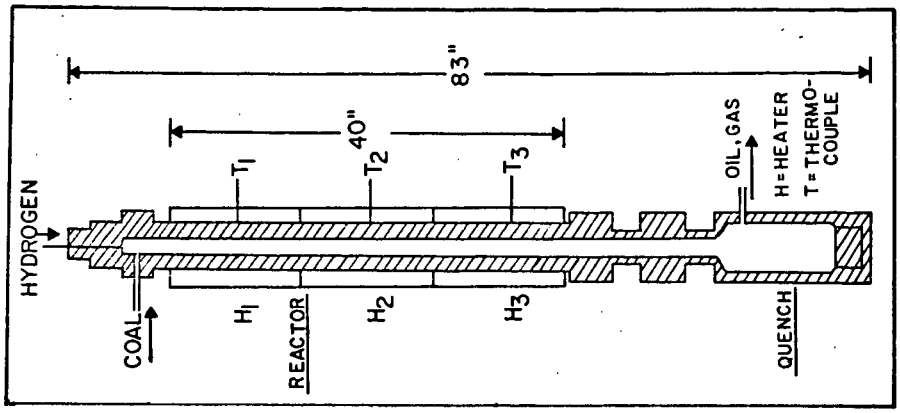

FIGURE 2. O.C.R. REACTOR AND QUENCH TANK.

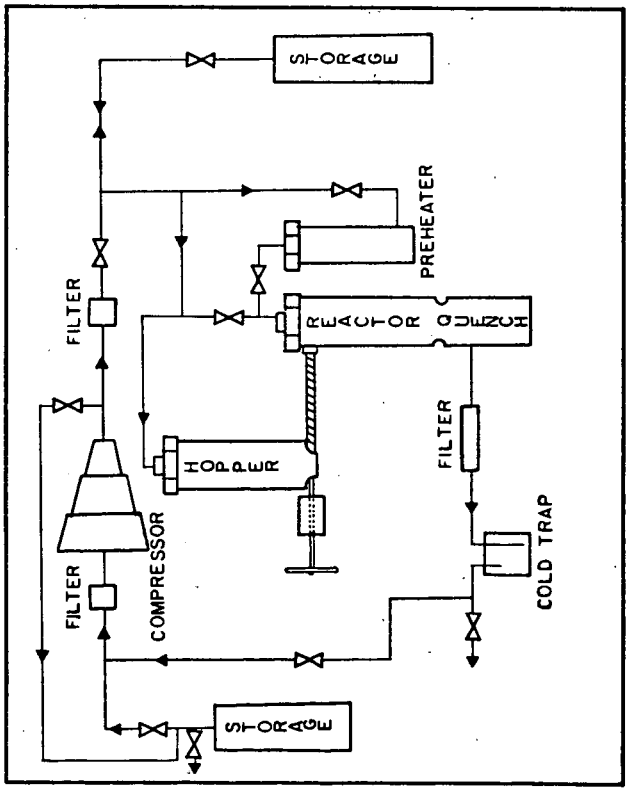

FIGURE 1. SCHEMATIC DIAGRAM OF O.C.R. FREE-FALL COAL HYDROGENATION UNIT.

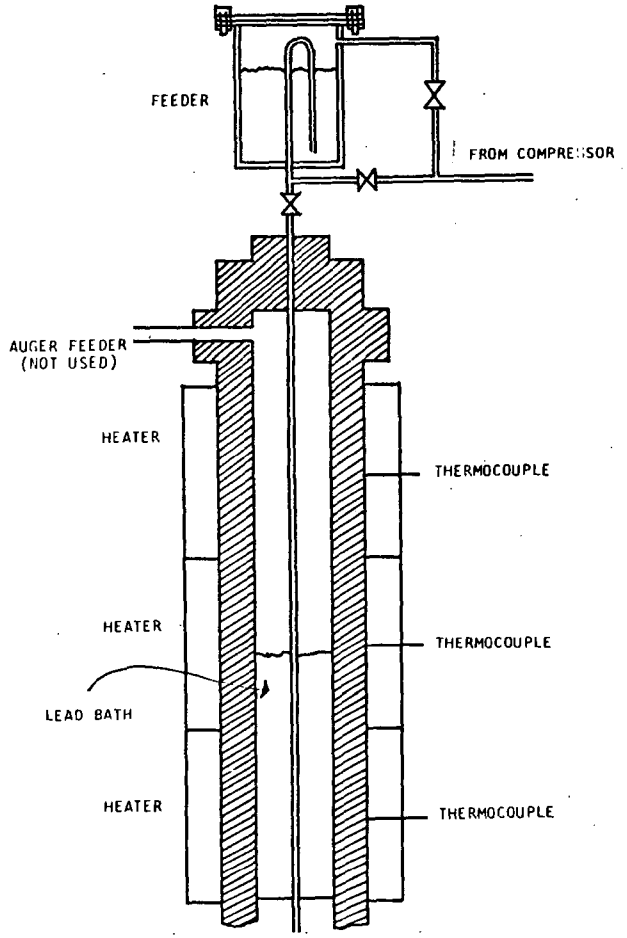

FIGURE 3. FLUIDIZED FEEDER WITH 1/8 INCH REACTOR.

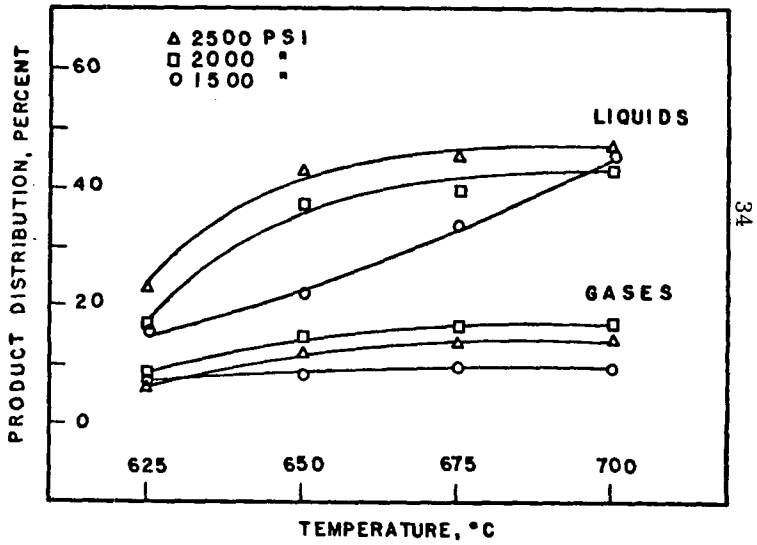

FIGURE 4. PRODUCT DISTRIBUTION FOR A REACTIVE (ORANGEVILLE, UTAH) COAL.

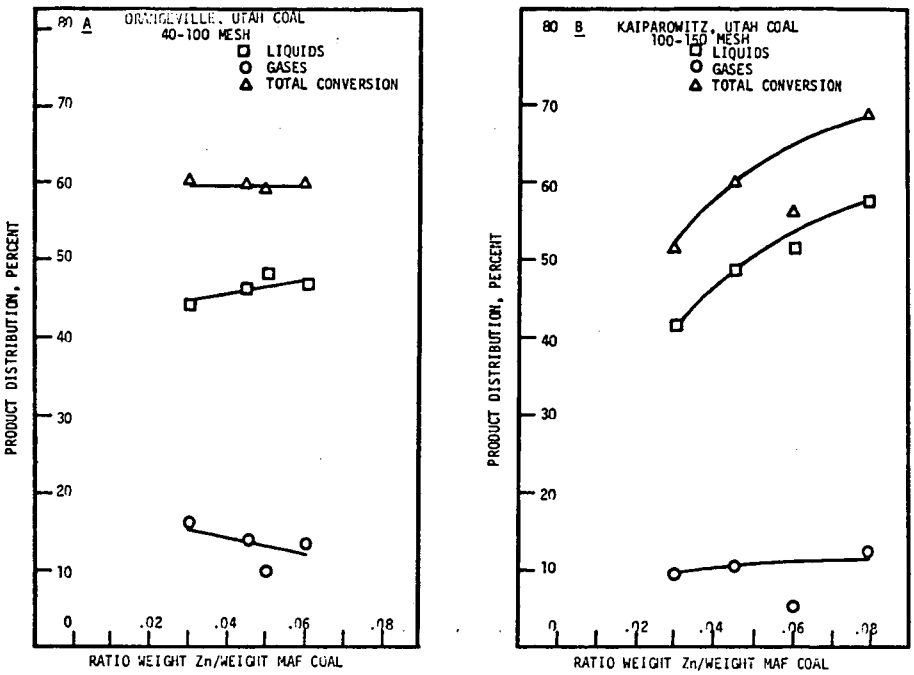

FIGURE 5. EFFECT OF CATALYST CONCENTRATION ON COAL CONVERSION

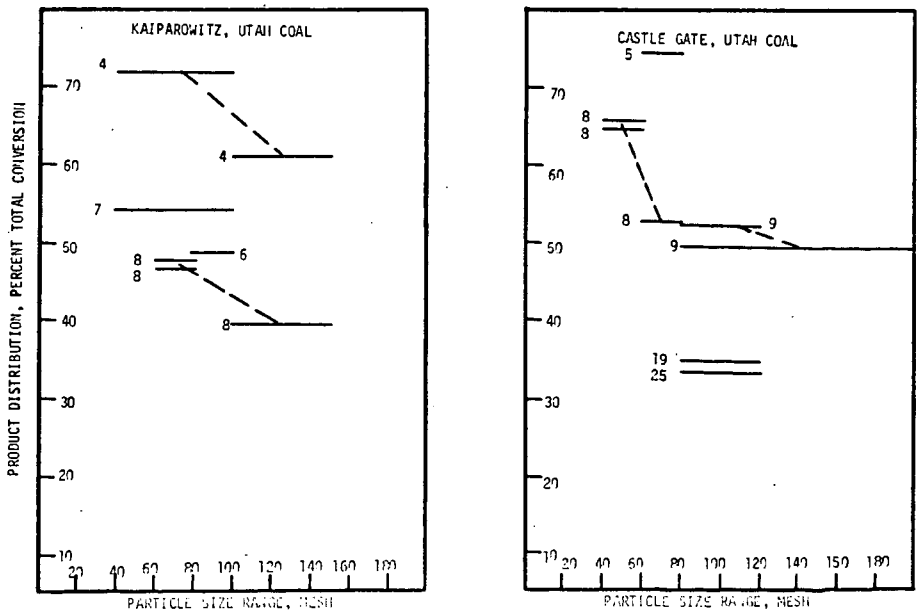

FIGURE 6. EFFECT OF PARTICLE SIZE AND FEED RATE ON CONVERSION OF COAL

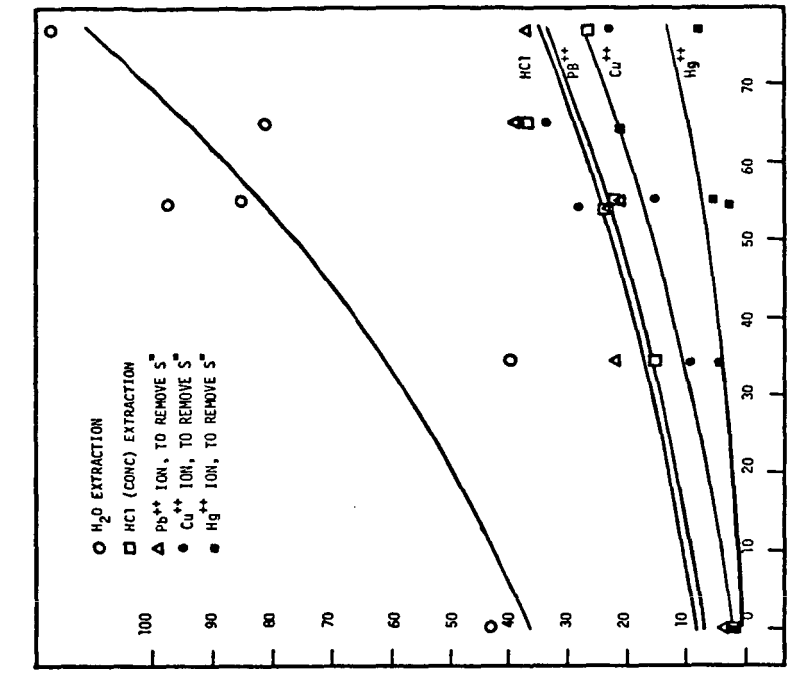

FIGURE 8. EXTRACTION OF ZINC FROM CHAR FOLLOWING COAL HYDROGENATION

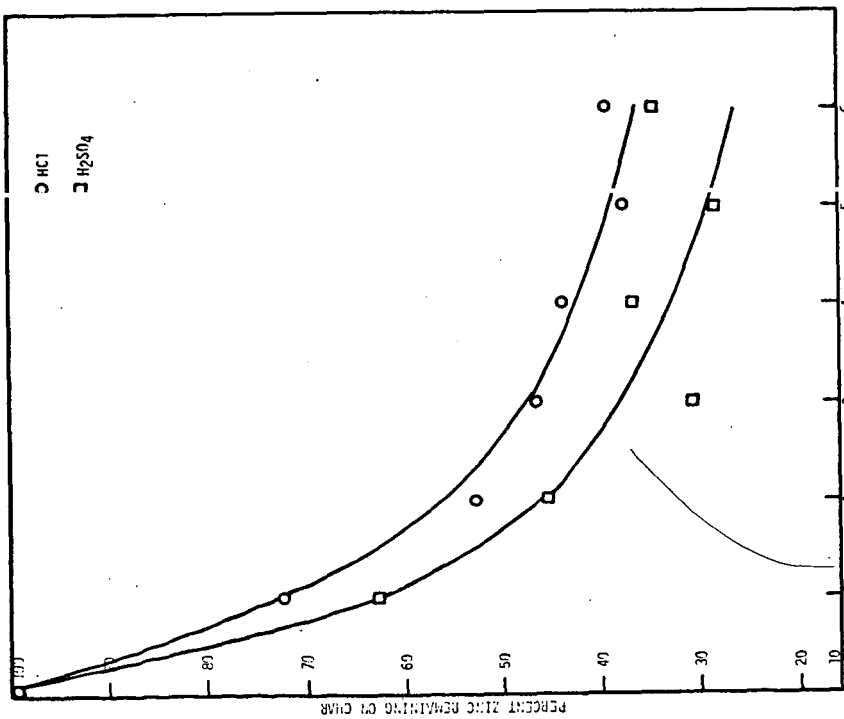

FIGURE 7. EXTRACTION OF ZINC FROM CHAR USING SUCCESSIVE PORTIONS OF 1 NORMAL HCL AND H_2SO_4

CONVERSION OF BOVINE MANURE TO OIL

Y. C. Fu, S. J. Metlin, E. G. Illig, and I. Wender

Pittsburgh Energy Research Center, U. S. Department of the Interior, Bureau of Mines, 4800 Forbes Avenue, Pittsburgh, Pennsylvania 15213

INTRODUCTION

Agriculture is the biggest source of wastes in the United States. Livestock on American farms produce over 2 billion tons of manure each year (approximately 400 million tons of organic matter), and these animal wastes are becoming a pollution, odor, and health problem. Efforts are being made by the Bureau of Mines to develop better and more efficient disposal methods using pyrolysis (1) and combustion (2) techniques. Animal waste is also a vast, untapped potential energy source if it can be converted to fuel.

Organic solid wastes, including urban refuse, agricultural wastes, sewage sludge, and bovine manure can be converted to oil by reaction with carbon monoxide and water at temperatures of 350° to 400°C and pressures near 4000 psig (3,4). The present work deals more extensively with the conversion of bovine manure to oil, and investigates effects of using synthesis gas (H_2:CO = 0.9:1) or hydrogen in place of carbon monoxide, and of adding catalyst and vehicle. It shows that synthesis gas can be used in place of carbon monoxide to convert manure to oil in reasonably good yield. Significant process improvements, such as low operating pressure and less energy requirement for heating, are achieved by the use of water:manure ratio as low as 0.25:1 with a suitable high boiling vehicle.

EXPERIMENTAL

The conversion of manure to oil with carbon monoxide and water was studied in a 1-liter magnetically-stirred stainless steel autoclave. Bovine manure from three sources was used. In the temperature range of 300° to 400°C, the operating pressure ranged from 2400 to 5300 psi. Most of these experiments were carried out for 0.5 to 1 hour at the reaction temperature. After the experiment, rapid internal cooling of autoclave to ambient temperature was achieved. Gaseous products were analyzed by mass spectrometry, and heavy oil products containing residue were separated from water and extracted by benzene to determine the amounts of the oil and the residue. The conversion of organic matter in manure was obtained by subtracting the weight percent of residue (excluding ash) from 100. Data on oil yield and carbon monoxide consumption were given on the basis of moisture-ash-free manure.

No catalyst was added for the conversion of manure with carbon monoxide and water. But in some runs using hydrogen or synthesis gas (H_2:CO = 0.9:1) in place of carbon monoxide, hydrogenation catalysts were used in an attempt to improve oil yield and hydrogen utilization.

RESULTS AND DISCUSSION

As shown in Table 1, both conversion and oil yield increased with temperature in the 300° to 380°C range, and the organic matter in bovine manure was almost completely converted by the reaction with carbon monoxide and water at 380° and 400°C. The variation in carbon monoxide consumption correlates well with the oil

yield as shown in Figures 1 and 2 and is in the range of 0.7 to 0.8 gram/gram manure at the best conversion. Figure 2 also shows that there is no increase in oil production or carbon monoxide consumption after 15 minutes reaction time at 380°C. The unconverted residue was inorganic, mostly silica. The extent of gas evolution owing to the thermal decomposition of manure appeared to be minor based on carbon balance in the gas phase, but the net weight increase in the gas phase amounted to as much as 37 weight percent on the organic manure basis at 400°C, because of the oxygen removal from manure to form carbon dioxide and concurrent water-gas shift reaction to form carbon dioxide and hydrogen. In addition, substantial amounts of water-soluble compounds were present in the yellowish water layer. On standing in the air, the solution darkened and a precipitate formed. The aqueous solution was evaporated to dryness and the residue was analyzed by infrared spectroscopy. Strong bands in the 1600 cm^{-1} region (corresponding to formates and acetates) were observed.

TABLE 1. Effect of temperature on conversion of bovine manure (maf basis)

(manure[a] as received 40 g, water 160 g, 600 psi initial CO pressure, 1 hour reaction time)

Temp, °C	Operating pressure, psi	Conversion, percent	Oil yield, percent	Weight increase in gas phase, percent of manure	CO consumption, g/g manure
300	2440	79	14	20	0.13
350	3650	95	30	25	0.41
380	4780	99	38	35	0.70
400[b]	5300	99	38	37	0.81

[a] For analysis of manure, see Table 2.
[b] Reaction time is 30 minutes.

The analysis of manure and its products in Table 2 shows that treatment of manure with carbon monoxide and water results more in oxygen removal than in hydrogen addition. The hydrogenation effect is not apparent from the product analysis, because the starting manure probably contains many hydroxyl groups which contribute to the hydrogen content. Elemental analysis of the oil product did not vary significantly between 300° and 400°C. The oil product obtained at 380°C has a softening point below room temperature, a kinematic viscosity in the range of 520 to 580 centistokes at 60° C, and a heating value of 16,240 Btu per pound.

TABLE 2. Analysis of bovine manure and oil products, percent

	Manure[a]		Oil			
	As used[b]	maf basis	400°C	380°C	350° C	300°C
C	41.2	52.0	79.8	80.4	79.5	77.4
H	5.7	6.7	9.1	9.4	9.5	9.8
N	2.3	2.9	2.7	3.0	3.1	2.9
S	0.3	0.3	0.20	0.26	0.24	0.27
O (by diff.)	33.3	38.1	8.2	7.1	7.7	9.6
Ash	17.2	--	--	--	--	--
H/C atomic ratio		1.55	1.37	1.40	1.43	1.52

[a] Cow manure, Midwest Research Institute, Kansas City, Missouri.
[b] Moisture = 3.6 percent.

Use of hydrogen in place of carbon monoxide decreased the conversion and oil yield (Table 3). Synthesis gas (H_2:CO = 0.9:1) gave almost complete conversion but slightly lower oil yield than pure carbon monoxide, at a considerable reduction in the consumption of carbon monoxide. Some hydrogenation catalysts were used in an attempt to promote the utilization of hydrogen present in the gas phase. Cobalt molybdate appeared to have a favorable effect on the conversion of manure with hydrogen, but not when synthesis gas was used. When sodium carbonate was used with synthesis gas, a significant improvement in oil yield was obtained. An increase in autoclave pressure was also observed, indicating a greater degree of water-gas shift reaction as a result of the addition of sodium carbonate.

At a temperature of 450°C, significant improvements in oil product quality were observed in that the carbon content was increased, oxygen content was decreased, and viscosity was reduced (Table 4). The change in the oil product properties is accompanied by some decrease in the oil yield, mainly because the oxygen-containing groups are further reduced and/or removed. At this temperature, cobalt molybdate catalyst appears to have a beneficial effect in reducing the viscosity of the oil product. Hydrogen gave a more fluid product than synthesis gas.

The organic matter of manure contains about 40 percent oxygen which during the conversion process will be removed in the form of carbon dioxide, water, and water-soluble compounds. Based on our experience, we speculate that at best an oil yield of about 50 percent can be realized. Above experiments using water and carbon monoxide or synthesis gas have shown that the oil yield from manure is reasonable.

Water functions both as the reactant and vehicle. Water is the least expensive vehicle, but it has two economic disadvantages in a commercial process (1) operating pressure can become too high because of the high vapor pressure of steam at the reaction temperature, and (2) a large amount of energy is required to heat and vaporize water. Some experiments were carried out using only small amounts of water in the presence of a low-vapor pressure and less energy-requiring vehicle. An alkylnaphthalene-based oil (boiling above 235°C) was used as the vehicle. The results in Table 5 indicate that the water:manure ratio can be reduced to as low as 0.25:1 while giving 83 percent oil product yield based on feed of maf manure plus vehicle. As discussed earlier, if one assumes that only 50 percent of organic matter in manure can be converted to oil, the maximum obtainable oil product yield based on maf manure plus vehicle would be 87.5 percent. If we assume a 98 percent recovery for the vehicle as we found in a blank run, the above 83 percent yield based on feed would be equivalent to 38 percent oil yield based on maf manure. The operating pressure is also reduced significantly as the water:manure ratio is decreased. This reduction in pressure and use of a vehicle oil (generated in the process) significantly decrease the high capital investment and operating cost of the manure to oil process.

REFERENCES

1. M. D. Schlesinger, W. S. Sanner, and D. E. wolfson. Proc. Agr. Food Chem., Am. Chem. Soc., Sept. 1972.
2. E. G. Davis, I. L. Feld, and J. H. Brown. Bureau of Mines Tech. Prog. Rept. 46 (1972).
3. H. R. Appell, Y. C. Fu, S. Friedman, P. M. Yavorsky, and I. Wender. Bureau of Mines Rept. Inv. 7560 (1971); Agr. Eng., pp. 17-19, Mar. 1972.
4. S. Friedman, H. H. Ginsberg, I. Wender, and P. M. Yavorsky. Third Mineral Wastes Utilization Synposium, IIT, Mar. 1972.

TABLE 3. Effects of hydrogen or synthesis gas[a] on conversion

(160 g water, 40 g manure as received, 2 g catalyst, 600 psi initial pressure, 1 hour at 380°C)

Gas	Catalyst	Operating pressure, psi	Conversion, percent	Oil yield, percent	Weight increase in gas phase, percent of manure	CO consumption, g/g manure
H_2	--	4500	83	21	18	--
H_2	$SnCl_2$	4360	81	22	19	--
H_2	CoMo	4540	90	27	22	--
H_2 + CO	--	4740	99	34	30	0.41
H_2 + CO	CoMo	4680	99	33	28	0.40
H_2 + CO	Na_2CO_3	4790	99	38	35	0.48
H_2 + CO	CoMo + Na_2CO_3	4770	99	38	35	0.47

[a] H_2:CO = 0.9:1.

TABLE 4. Conversion of steer manure[a] at 450°C (maf basis)

(reaction time = 0.5 hour)

Gas	H_2	H_2 + CO[b]	H_2 + CO[b]
Water:manure	0:1	1:1	1:1
Catalyst[c]	CoMo	CoMo	--
Operating pressure, psi	3700	4150	4200
Conversion, percent	99	99	99
Oil yield, percent	15	22	21
Oil analysis,			
C	85.3	82.6	81.3
H	8.8	8.4	8.5
N	3.6	6.0	6.9
S	0.33	0.33	0.24
O (by diff.)	1.97	2.67	3.06
H/C atomic ratio	1.24	1.22	1.25
Kinematic viscosity of oil at 60°C, centistoke	10	133	252

[a] Texas steer manure; analysis, percent: C = 25.5, H = 4.0, N = 2.6, S = 0.4, O = 22.8, ash = 44.7, moisture = 5.7.
[b] H_2:CO = 0.9:1.
[c] 3.3 parts per hundred parts manure.

TABLE 5. Effect of vehicle

(1000 psi initial synthesis gas[a] pressure, 380° C)

Water:manure[b]:vehicle[c]	1:1:2.5	0.5:1:2.5	0:25:1:2.5	0.25:1:2.5
Catalyst	--	--	Na_2CO_3	--
Operating pressure, psi	3400	3100	2800	3300[d]
Time, hr	0.5	0.5	1	0.5
Conversion, percent	94	91	95	89
Oil product yield, percent feed[e]	84	83	83	82

[a] H_2:CO = 0.9:1.
[b] Beef cattle manure, Beltsville, Md.; analysis, percent: C = 44.7, H = 6.4, N = 3.0, S = 0.37, O = 37.2, ash = 8.3, moisture = 5.9.
[c] An alkylnaphthalene-based oil, Sunoco.
[d] 1260 psi initial pressure.
[e] Based on feed of maf manure plus vehicle.

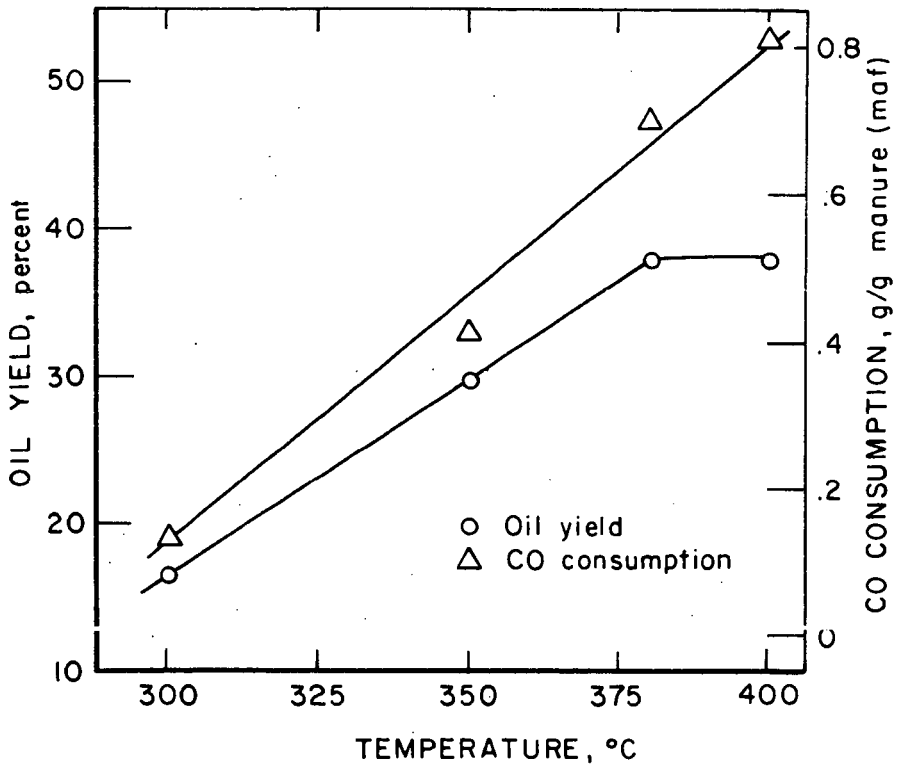

Figure 1 - Effect of temperature on oil yield and CO consumption at 1 hour reaction time.

4-24-72 L-12857

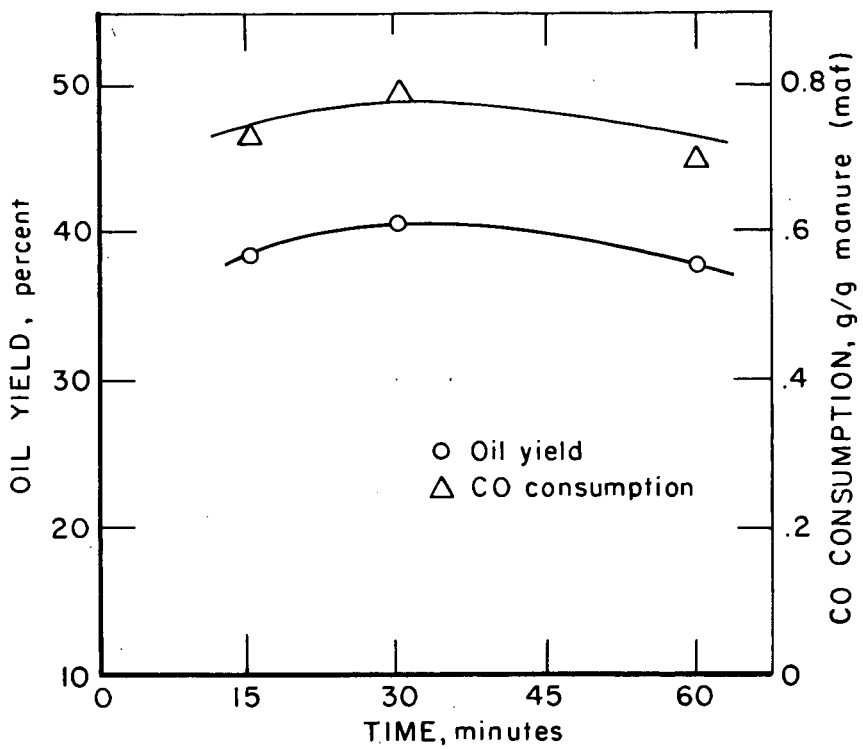

Figure 2 – Effect of reaction time on oil yield and CO consumption at 380°C.
4-24-72 L-12858

PREPARATION OF ASH-FREE, PYRITE-FREE COAL BY MILD CHEMICAL TREATMENT

Leslie Reggel, Raphael Raymond, Irving Wender, and Bernard D. Blaustein

Pittsburgh Energy Research Center, U. S. Department of the Interior,
Bureau of Mines, 4800 Forbes Avenue, Pittsburgh, Pennsylvania 15213

The major fraction of the electricity generated in the United States is produced by coal-fired power plants, and the demand for electricity is increasing rapidly. Low-sulfur coals meeting air pollution specifications for utility use are in short supply in the eastern part of the country. Low-sulfur fuel oils which are also used to generate electricity are limited in domestic supply, are costly, and usually must be obtained from foreign sources. Removal of sulfur from coal, either before, during, or after combustion (i.e., removal of sulfur oxides from stack gas), to meet air quality standards, is therefore one of the most pressing needs in the related fields of energy and clean environment. Numerous processes for sulfur removal are being actively investigated by many organizations, including the Bureau of Mines of the U. S. Department of the Interior.

Sulfur in coal occurs as sulfate; as pyrite, FeS_2; and as organic sulfur which is part of the coal structure. The sulfate is usually low. In experiments being carried out at the Pittsburgh Energy Research Center of the Bureau of Mines, almost all of the pyritic sulfur has been removed from some coals by treatment with aqueous alkali. For example, 30 g of -200 mesh Illinois No. 6 high volatile B bituminous coal is treated with a solution of 24 g of sodium hydroxide in 240 ml of water for 2 hr at 225° in a stirred autoclave, followed by acidification of the coal-aqueous alkali slurry with carbon dioxide. (The solution of sodium hydroxide used is referred to as "10% aqueous NaOH" in the tables.) In this treatment, the pyritic sulfur is removed, but the organic sulfur in the coal is not attacked by this procedure; for some coals, removal of pyritic sulfur would give a product that meets present specifications for sulfur content for use in power plants. The solid product obtained by this experimental procedure has a somewhat higher ash content than does the original coal. However, if the sodium hydroxide treatment is followed by acidification with dilute hydrochloric acid (instead of carbon dioxide), most of the mineral matter originally present is removed from the coal. The starting Illinois No. 6 coal contains 9.6% ash and 1.1% pyritic sulfur; the product contains 0.7% ash and 0.1% pyritic sulfur. The yield of coal is 91.5% (maf basis).

Table 1 gives the results of various experiments with Illinois No. 6 coal. The organic sulfur is reported on a moisture- and ash-free basis, since removal of ash and/or pyrite will concentrate the organic sulfur and make it seem to increase. It is noted that in some runs the organic sulfur does increase, even on an maf basis, and even allowing for the fact that the analysis is by difference and subject to an inherently large (but uncertain) error.[1]

[1]Organic sulfur in coal cannot be determined by any direct method. The standard procedure is to determine total sulfur, sulfate sulfur, and pyritic sulfur. The sulfate sulfur and the pyritic sulfur are subtracted from the total sulfur and the remainder is assumed to be organic sulfur. In an indirect method such as this, the probable error of the organic sulfur must be larger than the largest probable error of the three values from which it is derived.

TABLE 1. Illinois No. 6 (River King) hvbb coal: effect of 10% aqueous NaOH for 2 hr at 225°, followed by various acid workups, on ash and sulfur content (analyses on dry basis)

Run 11R-	Treatment	Workup	Ash	S total	S sulfate	S pyritic	S organic (diff., maf)
37	None	-	9.8	3.26	0.21	1.08	2.19
37A	NaOH	CO_2	12.4	2.05	0.11	0.13	2.06
83A	NaOH	CO_2	12.2	2.25	0.18	0.16	2.17
93	None	-	9.82	3.27	0.31	1.05	2.12
96	$Ca(OH)_2$	HCl	8.16	3.04	0.04	1.04	2.14
97	NaOH	HCl	0.67	2.54	0.01	0.11	2.44
103	None	-	9.77	3.30	0.33	0.92	2.28
103A	NaOH	HCl	0.84	2.58	0.00	0.09	2.51
110	None	-	9.85	3.28	0.42	0.93	2.14
110A	H_2O	CO_2	9.46	2.77	0.01	0.98	1.96
111A	H_2O	HCl	8.76	2.85	0.01	1.04	1.98
112	None	-	9.84	3.20	0.42	0.96	2.01
112A	NaOH	SO_2	0.72	2.40	0.23	0.19	1.99
113A	NaOH	H_2SO_4	0.52	2.75	0.24	0.19	2.33
133	None	-	12.58	3.69	0.09	1.39	2.53
133A	NaOH	Aspirate; H_2SO_4 slowly	0.85	2.99	0.17	0.12	2.73
134	NaOH	Aspirate; H_2SO_4 slowly	0.59	2.96	0.20	0.18	2.59
135	NaOH	Aspirate; H_2SO_4 dropwise	0.91	2.82	0.09	0.16	2.59
136	30% NaOH	Aspirate; H_2SO_4 dropwise	0.87	2.84	0.07	0.06	2.73

The erratic increase in organic sulfur mentioned above is puzzling. It is possible that elemental sulfur is precipitated either at some stage of the reaction, or during the workup of the product; free sulfur would be reported as organic sulfur in the standard analytical procedure for sulfur forms. (In a modification of the standard procedure, where the organic sulfur is determined by taking the residue from the pyrite determination and analyzing for sulfur, free sulfur would also be reported as organic sulfur.) An attempt was made to settle this question by extraction (Soxhlet) of a coal sample with ethanol, and analysis of the extract for sulfur by ultraviolet spectrometry; no sulfur was found. It is also possible that at some point in the procedure, free sulfur or polysulfide ion is formed and attacks the coal, giving an actual increase in organic sulfur.

One possible method of preventing an increase in organic sulfur would be to remove the sulfide-containing alkali solution from contact with the coal before any work-up is done. (This assumes that the troublesome sulfur material is in solution and is not already adsorbed on the coal surface.) This technique, using a filter stick, has been used on those runs which are marked (in the tables) as "aspirate." This aspiration procedure removes about 70-90% of the alkaline solution. Obviously, in any commercial procedure, filtration, centrifugation, or some other process would be used in order to recover caustic solution for re-use, to minimize the amount of acid needed, and also to recover minerals and sulfur dissolved in the alkali.

There is some evidence that the aspiration of the caustic results in less of an increase of organic sulfur (table 1, run 113A compared with runs 133A, 134, 135). There is also evidence that aspiration results in better removal of ash and pyrite (table 2, runs 119A and 121A).

TABLE 2. Elliot mine mvb coal: effect of 10% aqueous NaOH for 2 hr at 225°, followed by various workups, on ash and sulfur content (analyses on dry basis)

Run 11R-	Treatment	Workup	Ash	S total	S sulfate	S pyritic	S organic (diff., maf)
99	None	-	18.15	4.31	0.20	3.25	1.05
99A	NaOH	CO_2	22.84	2.27	0.19	0.19	2.44
104	None	-	18.21	4.31	0.26	3.29	0.93
104A	NaOH	HCl	5.11	3.61	0.01	1.94	1.75
114	None	-	19.86	5.21	0.32	3.74	1.44
114A	NaOH	HCl (special)	4.06	4.06	0.01	2.39	1.73
115A	NaOH, 7 hr	HCl	5.84	3.88	0.10	2.08	1.81
116A	30% NaOH	HCl	3.03	3.16	0.03	0.75	2.45
117A	NaOH, 325°	HCl	8.43	2.77	0.04	0.48	2.46
119-1	None	-	19.68	5.23	0.35	3.85	1.28
119A	NaOH	H_2SO_4	7.26	5.21	0.06	3.35	1.94
120A	NaOH	H_2SO_4 (special)	4.56	4.38	0.14	2.46	1.85
121A	NaOH	Aspirate; H_2SO_4	6.06	3.79	0.07	2.54	1.25
122A	NaOH	Aspirate; H_2SO_4 (special)	4.07	3.52	0.19	1.97	1.41
126A	Double volume 10% NaOH	Aspirate; H_2SO_4	5.24	3.49	0.13	1.86	1.58

The use of sulfur dioxide for the acidification step (table 1, run 112A) gave good results, suggesting that it might be possible to use sulfur oxides from stack gas for the process. It is noteworthy that sulfur dioxide is a strong enough acid to cause the deashing reaction to take place, but carbon dioxide is not effective for deashing.

The chemistry of the dissolution of pyrite in aqueous alkali is not known, but something can be suggested with regard to the deashing reaction. The following mechanistic scheme is based upon the reactions which take place in purification of alumina from bauxite ore. When a coal is treated with alkali, the clay minerals probably dissolve and then precipitate as a stable insoluble sodium aluminum silicate of composition $3Na_2O \cdot 3Al_2O_3 \cdot 5SiO_2$. This is not soluble in alkali but is soluble in strong acid. Thus, after acidification, the silica, alumina, and some other mineral matter of the coal should be found mostly in the acid fraction, with only a small amount in the alkaline fraction. Preliminary analytical data confirm this hypothesis.

In table 3, runs 124A and 125A give the results of alkali deashing-depyriting in the presence of hydrogen. The coal itself had a somewhat different behavior during workup; it tended to float during centrifugation. There was no uptake of gas and the results were similar to runs made under similar conditions in the absence of hydrogen (table 2). Further experiments are desirable, since the runs using

hydrogen gave relatively low ash and pyrite values. Run 128A was done in the presence of 1700 psi initial pressure of synthesis gas (0.9 H_2:1 CO). At the end of the reaction, the aqueous layer had a pH of about 5. It is obvious that the carbon monoxide reacted with the sodium hydroxide to give sodium formate. Analysis of the gases showed that 0.58 mole of carbon monoxide was used up, corresponding well to the 0.60 mole of sodium hydroxide initially present; the calculation also indicated the formation of 0.15 mole of hydrogen. Removal of pyrite is good (82% removed) but removal of ash is poor (only 49% removed). This suggests two possibilities. With neutralization of the sodium hydroxide via the formation of sodium formate, ash removal must be a relatively slow reaction or may require a fairly high alkali concentration, so that rate of mineral conversion becomes very slow after a short time. On the other hand, rate of pyrite reaction with sodium hydroxide must be fairly rapid, or else continues even in weak alkali, so that the final pyrite removal is still good. Another possibility, but a rather unlikely one, is that some of the pyrite is dissolved not by the alkali but by the formic acid. Pyrite is not soluble in dilute hydrochloric acid, but formic acid is a reducing agent, which may have some effect upon the pyrite.

TABLE 3. Effect of various gases in the presence of 10% aqueous NaOH, followed by acid workup, on the ash and sulfur of coal (dry basis)

Run 11R-	Coal	Treatment	Workup	Ash	S total	S sulfate	S pyritic	S organic (diff., maf)
119-1	Elliot	None	-	19.68	5.23	0.35	3.85	1.28
124A	Elliot	H_2, NaOH 250°	H_2SO_4	3.72	2.48	0.08	0.64	1.84
125A	Elliot	H_2, NaOH, 250°	H_2SO_4	3.39	2.26	0.02	0.29	2.02
128A	Elliot	H_2 + CO, NaOH, 250°	Aspirate; H_2SO_4	10.03	2.41	0.06	0.69	1.85
133	River King	None	-	12.58	3.69	0.09	1.39	2.53
137	River King	Air, NaOH, 225°, 1 hr	Aspirate; H_2SO_4	14.27	2.10	0.05	0.21	2.16

Run 137 in table 3 shows the effect of air (760 psi at room temperature) upon the reaction of River King coal with sodium hydroxide. There was an uptake of oxygen. The aspirate had a pH of 5.5-6.0 (probably bicarbonate with dissolved carbon dioxide) and the oxygen content of the coal increased from 9.66 to 10.37%. Probably the oxygen and alkali oxidized some of the coal to "humic acids," using up the alkali in this reaction. The ash content increased, the pyritic sulfur decreased, but the sulfate was almost unchanged. The results suggest that the pyrite was rapidly attacked and converted to water-soluble sulfate; this is substantiated by the observation that during the acidification of the treated coal, there was no odor of either hydrogen sulfide or sulfur dioxide, though there was copious evolution of an odorless gas, presumably carbon dioxide. The organic sulfur (moisture- and ash-free basis) decreased from 2.53 to 2.16%. Since the increase in oxygen content of the coal would decrease the organic sulfur by dilution, these figures can be put on a moisture-, ash-, and oxygen-free basis; the change is then from 2.84 to 2.46% organic sulfur. This decrease in organic sulfur is small and probably subject to a fairly large analytical error; however, it does seem to be significant, in view of the fact that the organic sulfur tends to increase slightly in most other experiments.

One run (table 1, run 96) was made using aqueous calcium hydroxide, which would be a cheaper source of alkali than sodium hydroxide. The pyritic sulfur was not attacked; possibly this is because of the very limited solubility of calcium hydroxide, resulting in a very low concentration of hydroxide ion in solution.

Treatment of the coal with water at 225° (conditions used for the alkali treatment) did not have any effect; thus, there is no doubt that the deashing requires alkali and is not simply a result of a hydrothermal water treatment. This was shown to be true for both carbon dioxide workup and hydrochloric acid workup (runs 110A and 111A, table 1).

No further discussion of the results given in table 2 (Elliot mine mvb coal) and in table 4 (Indiana No. 5 hvbb coal) will be given here, except to point out that Indiana No. 5, like Illinois No. 6, has been converted to a low-ash, low-pyrite material.

TABLE 4. Indiana No. 5 hvbb coal: effect of 10% aqueous NaOH for 2 hr at 225°, followed by various acid workups, on ash and sulfur content (analyses on dry basis)

Run 11R-	Treatment	Workup	Ash	S total	S sulfate	S pyritic	S organic (diff., maf)
108	None	-	9.55	3.47	0.35	1.02	2.32
108A	NaOH	HCl	0.48	2.63	0.02	0.06	2.56
109A	NaOH	CO_2	10.57	2.35	0.16	0.13	2.31
141	None	-	9.42	3.46	0.50	0.94	2.23
141A	NaOH	Aspirate; H_2SO_4 with heating and stirring	0.72	2.56	0.20	0.15	2.23

The depyriting-deashing procedure usually increased the heating values of the coals somewhat, as would be expected. The free swelling index usually changed only slightly.

An ash-free, pyrite-free coal would have several important potential applications, which would depend on its cost and specific characteristics. Ash-free coal might simplify the process to produce synthetic high-Btu gas from coal. If it were cheap enough, ash-free, pyrite-free coal would be much preferred for combustion to generate electricity, either in conventional steam plants, gas turbines, or MHD generators. The use of ash-free, pyrite-free coal should extend the life of the catalyst used for the catalytic hydrodesulfurization of coal. An ash-free feed should simplify the process of converting coal to liquid fuels with the conventional coal hydrogenation catalysts, by eliminating the separation of oil from solid residues. Ash-free coal should also find uses as materials for the preparation of electrodes and other specialty carbon products.

Further studies of the many variables in this deashing-depyriting reaction are in progress, to develop technical and economic data required so that the applicability of the process for supplying low-sulfur fuel can be fully evaluated.